Resource

Cell

Efficient Intracellular Delivery of Native Proteins

Graphical Abstract

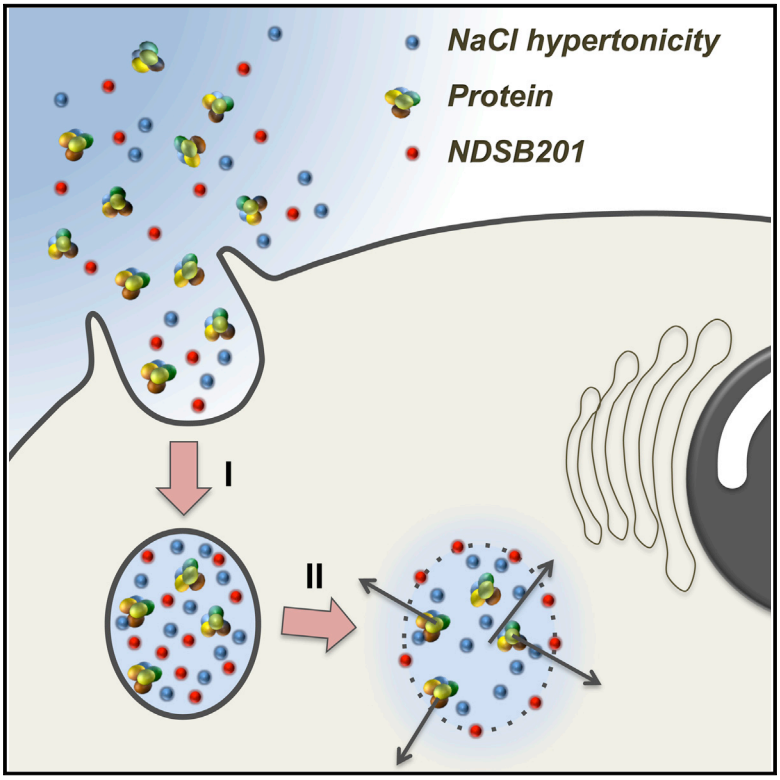

Authors

Diego S. D'Astolfo, Romina J. Pagliero, ..., Holger Rehmann, Niels Geijsen

Correspondence

n.geijsen@hubrecht.eu

In Brief

A small-molecule-based method called iTOP serves as an efficient method for the transduction of native proteins and other macromolecules into primary cells.

Highlights

- iTOP enables the intracellular delivery of macromolecules
- iTOP allows the highly efficient transduction of native proteins
- This protein transduction is independent of a transduction peptide sequence
- iTOP mediates efficient manipulation of a wide variety of primary cell types

D'Astolfo et al., 2015, Cell *161*, 674–690
April 23, 2015 ©2015 Elsevier Inc.
http://dx.doi.org/10.1016/j.cell.2015.03.028

CellPress

Cell

Efficient Intracellular Delivery of Native Proteins

Diego S. D'Astolfo,[1,2] Romina J. Pagliero,[2] Anita Pras,[1] Wouter R. Karthaus,[1,2] Hans Clevers,[1,2] Vikram Prasad,[3] Robert Jan Lebbink,[2] Holger Rehmann,[2] and Niels Geijsen[1,2,4,*]
[1]KNAW-Hubrecht Institute, Uppsalalaan 8, 3584 CT Utrecht, the Netherlands
[2]University Medical Center Utrecht, Heidelberglaan 100, 3584 CX Utrecht, the Netherlands
[3]Department of Molecular Genetics, Biochemistry, and Microbiology, University of Cincinnati College of Medicine, Cincinnati, OH 45267, USA
[4]Department of Clinical Sciences of Companion Animals, Faculty of Veterinary Medicine, Utrecht University, Yalelaan 108, 3584 CM Utrecht, the Netherlands
*Correspondence: n.geijsen@hubrecht.eu
http://dx.doi.org/10.1016/j.cell.2015.03.028

SUMMARY

Modulation of protein function is used to intervene in cellular processes but is often done indirectly by means of introducing DNA or mRNA encoding the effector protein. Thus far, direct intracellular delivery of proteins has remained challenging. We developed a method termed iTOP, for induced transduction by osmocytosis and propanebetaine, in which a combination of NaCl hypertonicity-induced macropinocytosis and a transduction compound (propanebetaine) induces the highly efficient transduction of proteins into a wide variety of primary cells. We demonstrate that iTOP is a useful tool in systems in which transient cell manipulation drives permanent cellular changes. As an example, we demonstrate that iTOP can mediate the delivery of recombinant Cas9 protein and short guide RNA, driving efficient gene targeting in a non-integrative manner.

INTRODUCTION

Modulation of protein function is a powerful means of intervention in disease. Protein manipulation is usually achieved indirectly, at the DNA or RNA level, either by "knockdown" or mutation of the encoding gene or by ectopic overexpression of wild-type or mutant genes. Transient, non-integrative modulation of cell function by direct intracellular delivery of proteins has appealing application, both in research and the clinic. However, the currently available toolset for the intracellular transduction of proteins is limited.

In 1982, Okada and Rechsteiner reported that brief hypertonic shock followed by a hypotonic treatment can induce the intracellular uptake of proteins into cells (Okada and Rechsteiner, 1982). Unfortunately, this technique proved limited to immortalized cell lines and yielded poor protein transduction efficiencies and poor cell survival in primary cells. The discovery of cell-penetrating peptides (CPPs) sparked renewed interest in protein-mediated cell manipulation. Independent discoveries from Green and Frankel demonstrated that the HIV TAT protein can transduce itself across the cell membrane (Schwarze et al., 2000). Nagahara and colleagues subsequently demonstrated that TAT-peptide-mediated protein transduction also worked when the TAT peptide was cloned as an in-frame fusion to a recombinant protein of interest, providing a tractable method for the transduction of recombinant proteins (Schwarze et al., 2000). CPP-mediated protein transduction appears to work with all cell types, but the dependence of physical fusion of the CPP with the cargo protein can disrupt protein function or alter the subcellular localization of the fusion protein (Lundberg and Johansson, 2001). Thus, the success of CPP-driven protein transduction is variable and dependent on the nature and physical properties of the protein cargo.

Here, we describe a method for the efficient delivery of native proteins and other macromolecules, such as small RNAs, into primary cells. We discovered that a combination of small molecules drives the highly efficient intracellular delivery of native proteins, independent of any transduction peptide. We termed this process "iTOP" for induced transduction by osmocytosis and propanebetaine. iTOP is an active uptake mechanism in which an NaCl-mediated hyperosmolality, in combination with a transduction compound (a propanebetaine), triggers macropinocytotic uptake and intracellular release of extracellularly applied macromolecules. We demonstrate that iTOP allows the highly efficient delivery of recombinant cytoplasmic and nuclear proteins into a wide variety of primary cell types. Finally, we demonstrate that iTOP of recombinant Cas9 protein and in-vitro-transcribed short guide RNA provides a highly efficient and non-integrative means of gene editing.

RESULTS

Transduction of Native Protein Independent of a Cell-Penetrating Peptide

Protein transduction provides an attractive means to transiently manipulate cell behavior without risk of permanent changes to the cell's genome. We set up a system for protein transduction into cells by generating recombinant Oct4-VP16 protein with an N-terminal histidine tag (H6) and a C-terminal poly-arginine CPP (R11-CPP), to drive self-transduction of the protein across the cell membrane (Zhou et al., 2006) (Figure 1A). To validate the system, we also generated recombinant Oct4-VP16 protein

without the R11-CPP or without both the R11-CPP and histidine purification tags (Figure 1A, top). We used a firefly luciferase reporter plasmid containing six tandem Oct4 binding sites (Tomilin et al., 2000) to measure intracellular activity of transduced Oct4 protein (Figure 1A, bottom). Luciferase activity was measured 12 hr after adding the recombinant Oct4 protein. Transduced H6-Oct4-VP16-R11 protein activated the Oct4-luciferase reporter in a dose-dependent manner (Figure 1B). Surprisingly, addition of the H6-Oct4-VP16 protein (without R11-CPP) or Oct4-VP16 protein (without R11-CPP and H6 tag) elicited the same response (Figure 1B). This finding was highly unexpected, yet the dose-dependent activation of the Oct4 reporter suggested that Oct4 protein was incorporated into the cells independent of the CPP sequence.

We hypothesized that one or more components of the buffer in which we purified the recombinant protein were responsible for the CPP-independent protein transduction. To test this, we examined the effect of omitting individual components of the buffer on Oct4 transduction. As shown in Figure 1C, Oct4-luciferase reporter activation was abrogated when either NaCl or non-detergent Sulfobetaine-201 (NDSB-201) was omitted from the buffer, indicating that a combination of NaCl and NDSB-201 is required for the introduction of Oct4 protein into cells. Because omission of either compound could potentially affect Oct4 protein solubility, it is important to note that the absence of NaCl or NDSB-201 did not result in Oct4 protein precipitation from the solution (data not shown). To exclude the possibility that luciferase reporter activation occurred through an Oct4-protein-independent manner, we also analyzed the effect of the Oct4 protein on a luciferase reporter without Oct4 binding sites. As shown in Figure S1A, the Oct4 protein did not activate the luciferase reporter without Oct4 binding sites, demonstrating that the observed effect was indeed dependent on binding of the transduced Oct4 protein to the target sites. Oct4 specificity was further confirmed using a tandem Oct4-Sox2 reporter (Boyer et al., 2005) and recombinant Oct4 protein synergized with Sox2, again demonstrating its functional specificity (Figure S1B).

Effect of Osmolality, NDSB-201, Time, and Protein Concentration

To further examine the protein transduction parameters, we set up a more direct detection system to quantify transduced protein. We detected intracellular beta-lactamase, a small highly soluble protein (Figures S1C and S1D), using CCF2/AM, a non-fluorescent lipophilic substrate that can readily cross the cell membrane (Figure 1D, see Experimental Procedures). Once in the cytosol, CCF2/AM is cleaved by cytosolic esterases, which activate its fluorescence and leave the now negatively charged form, CCF2, trapped inside the cell. Upon excitation at 409 nm, CCF2 emits (green) light at 520 nm. Cleavage of CCF2 by intracellular beta-lactamase results in a shift in the emission wavelength to blue (447 nm). Thus, the ratio of blue versus green signal accurately quantifies intracellular beta-lactamase.

Using this assay, we explored the effect of time and/or NaCl, NDSB-201, and protein concentration on protein transduction of murine embryonic fibroblasts (MEFs). We discovered that optimal transduction time was directly proportional to the level of NaCl-induced hyperosmolality, with higher osmolalities resulting in faster protein transduction. Figure 1E integrates the effect of transduction time and different media osmolalities on beta-lactamase protein transduction. As control, beta-lactamase was transduced in isotonic media with addition of NDSB-201 (open squares). At 800 mOsmol/kg, transduction occurred rapidly (orange line) with optimal transduction time at 1.5 hr. In contrast, at 500 mOsmol/kg, transduction proceeded slowly, reaching optimal levels after 12 hr (red line). Intermediate osmolalities resulted in corresponding optimal transduction times as indicated (red and green lines). Extension of protein transduction time beyond the optimal timeframe was detrimental to the cells, resulting in lower transduction efficiency and cell death (Figure 1E, dashed lines).

We next tested whether other hypertonicity-inducing molecules could mediate protein transduction as well. As shown in Figure 1F, NaCl, RbCl, KCl, and LiCl all induced protein transduction at varying levels (Figure 1F). In addition, Na-gluconate supported protein transduction, indicating that the Cl^- anion in the added NaCl is dispensable for this process. In contrast, sucrose-, lactulose-, sorbitol-, and mannitol-induced hypertonicity did not support beta-lactamase protein transduction (Figure 1F). The above data demonstrate that protein transduction is critically dependent on hypertonicity induced by alkali metal cation-containing salts, especially Na^+ and Rb^+.

Next, we explored the effect of the NDSB-201 concentration on the beta-lactamase transduction. As shown in Figure 1G, beta-lactamase transduction was NDSB-201 dependent and most efficient at an NDSB-201 concentration of 10–25 mM NSDB-201. At high concentrations, NDSB-201 displays some toxicity, resulting in a decrease in protein transduction (Figure S1E).

Finally, we measured CCF2 cleavage as a function of beta-lactamase concentration. As shown, transduction of increasing concentrations of beta-lactamase protein for 3 hr in the presence of 25 mM NSDB-201 and NaCl-adjusted media (osmolality of 700 mOsmol/kg) resulted in increased intracellular beta-lactamase activity (Figure 1H, bars). Beta-lactamase transduction was not observed in the isotonic controls in the presence of 25 mM NSDB-201 (Figure 1H, open circles).

Altogether, this demonstrates that recombinant beta-lactamase protein is incorporated into the cell and released into the cytoplasm and is dependent on hypertonicity induced by Na^+- or Rb^+-containing salts, NDSB-201 concentration, transduction time, and extracellular protein concentration. We termed this process "iTOP" (*i*nduced *t*ransduction by *o*smocytosis and *p*ropanebetaine). Accurate determination of the amount of protein transduced into the cytosol is extremely challenging and is dependent on cell type, protein solubility, half-life, and the concentration at which it can be applied to the cells. Indeed, Figure 1H demonstrates a direct relationship between the extracellular concentration of beta-lactamase protein and the amount transduced into a cell. To provide a reference for the amount of transduced protein, we compared iTOP protein transduction to CCP-dependent protein delivery or the protein transduction method reported by Okada and colleagues. As shown, iTOP delivery is at least four times more efficient in transducing protein into primary fibroblasts than these previously reported methods (Figure S1F).

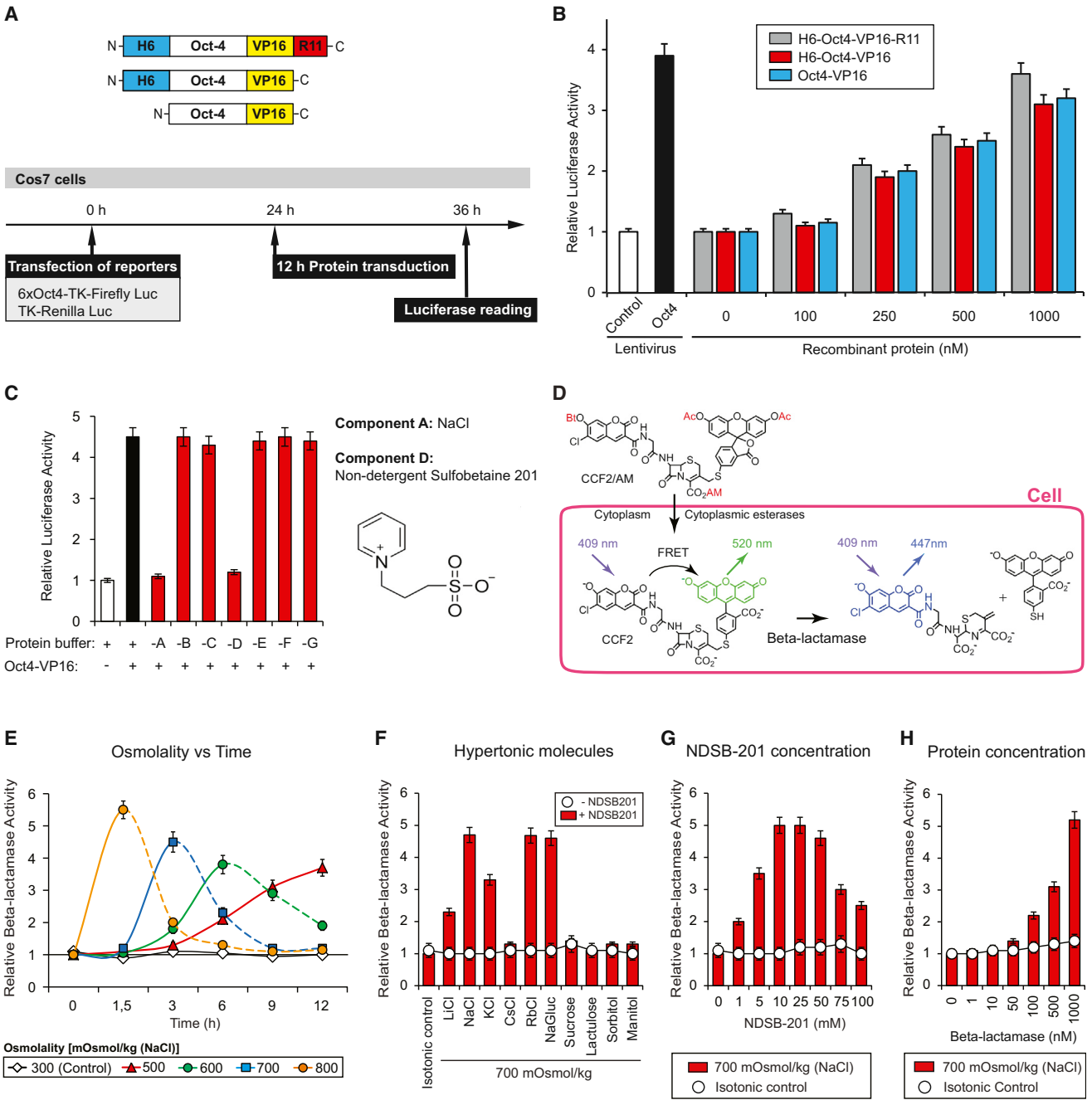

Figure 1. A Combination of NaCl Hypertonicity and NDSB-201 Induces Transduction of Native Proteins

(A) Top: schematic representation of the Oct4 recombinant proteins used in this study. Bottom: timeline of Oct4 protein transduction assay.

(B) Cos-7 cells were transfected with 6xOct4-TK-Firefly-Luc reporter and, 12 hr later, were transduced with increasing amount of Oct4 proteins as indicated. Firefly luciferase activity was normalized by co-transfection of Renilla luciferase construct. Controls were cells transduced with an empty or an Oct4-expressing lentivirus (white and black bars, respectively). Mean ± SD; n = 3.

(C) Cos-7 cells were transfected with 6xOct4-TK-Firefly-Luc reporter and incubated with Oct4-VP16 protein (Oct4 protein in elution buffer, 1:10 diluted in culture media, black bar) or without protein (white bar). Red bars represent cells transduced with Oct4-VP16 protein in the absence of one of the elution buffer components: A: NaCl (1 M), B: NaH_2PO4 (50 mM), C: Tris-HCl (50 mM), D: NDSB-201 (250 mM), E: 2-mercaptoethanol (100 μM), F: $MgCL_2$ (125 μM), and $ZnCl_2$ (125 μM). Firefly luciferase activity was normalized with co-transfected Renilla luciferase. Mean ± SD; n = 3.

(D) Schematic representation of the beta-lactamase reporter assay. The cell-permeable CCF2/AM compound is trapped in the cytoplasm by intracellular esterases, which convert it to the non-membrane-permeable, fluorescent CCF2. Excitation of CCF2 at 409 nm results in an emission signal at 520 nm (green signal). CCF2 cleavage by intracellular beta-lactamase abrogates intramolecular FRET, resulting in a shift in the emission wavelength to 447 nm (blue signal).

(legend continued on next page)

Protective Osmolytes Rescue Hypertonicity-Induced Cell-Cycle Inhibition

Although the combination of NaCl-induced hyperosmolality and NDSB-201 promoted efficient protein transduction, it also affected cell proliferation. Hyperosmotic stress is well known to induce cell-cycle arrest, followed by apoptosis in mammalian cells (Kültz et al., 1998). We observed by BrdU incorporation that protein transduction for 3 hr at 700 mOsmol/kg or for 12 hr at 500 mOsmol/kg reduces MEF proliferation by more than 60% compared to untreated cells, independent of the presence of beta-lactamase (Figure 2A). Apoptosis, measured by caspases 3/7 activity assay, was not detected in transduced cells (data not shown).

Osmoprotectants (or protective osmolytes) help cells cope with osmotic stress by accumulating in the cytosol, thereby balancing the osmotic difference between the intra- and extracellular environment. We tested whether the addition of osmoprotectants to media would prevent cell-cycle arrest during protein transduction. MEFs were treated with transduction media alone or supplemented with different osmoprotectants, and BrdU incorporation was measured as indicated in Figure 2B. In the absence of osmoprotectants, incubation of MEFs with transduction media reduced the cell proliferation rate to 34% compared to non-transduced controls (Figure 2B, red bar). The addition of osmoprotectants during transduction ameliorated this cell-cycle arrest to various degrees as shown in Figure 2B (green bars). The combination of glycerol and glycine was found most effective and almost completely prevented the hypertonicity-induced cell-cycle arrest, while still allowing protein transduction (Figure 2C). Unless otherwise indicated, we therefore included glycerol and glycine in subsequent protein transduction experiments.

To explore whether other cell types could similarly be transduced with minimal effect on cell proliferation, we transduced murine embryonic stem cells (mESCs) with beta-lactamase. mESCs appeared more sensitive to the hypertonic conditions. mESC transduction for 3 hr at 700 mOsmol/kg reduced cell proliferation even with added osmoprotectants glycine and glycerol (Figure 2D). We therefore examined whether lowering NaCl-mediated hypertonicity and extending transduction time (as shown in Figure 1E) would allow transduction of more sensitive cell types. Indeed, transduction of mESCs for 12 hr at 500 mOsmol/kg resulted in effective beta-lactamase transduction and minimal effect on cell proliferation (Figure 2D). In fact, it was possible to perform two subsequent rounds of beta-lactamase transduction with BrdU incorporation values of 75% compared to untreated cells (Figure 2E). Thus, a combination of NaCl-mediated hypertonicity, NDSB-201, glycine, and glycerol allows the transduction of native proteins with minimal effect on cell proliferation.

Efficient Protein Transduction in Multiple Primary Cell Types

To determine iTOP efficiency and the range of cell types that could be transduced using this method, we transduced Cre recombinase protein in mESC and other primary cells. We used mESCs containing a single copy of a Cre-activatable GFP-fluorescent reporter integrated in the Rosa26 locus (Srinivas et al., 2001). As outlined in Figure 3A, Cre-mediated removal of a loxP-flanked stop cassette activates a GFP reporter, allowing assessment of the percentage of successfully transduced cells in a population. mESCs were transduced with Cre protein at 500 mOsmol/kg for 12 hr. Increasing concentrations of recombinant Cre-protein resulted in increased percentage of GFP-positive (GFP+) cells (Figure 3B). One round of transduction with 10 μM of Cre protein activated the GFP reporter in 51% of the mESCs and increased to 79% after a second round of transduction (Figure 3B). To confirm that protein transduction did not affect mESC function, we tested the ability of transduced mESCs to form chimeras upon injection into recipient blastocyst embryos. Figure 3C shows an image of one of the chimeric mice, demonstrating that Cre protein transduction does not affect mESC pluripotency. Chimeric mice were able to generate offspring, demonstrating that Cre-transduced mESCs contributed to the germline (Figure 3D).

We next explored Cre recombinase protein transduction in multiple murine primary cell types isolated from mice carrying one copy of a lox-mRFP-lox-mGFP reporter. Single Cre protein transduction for 12 hr at 500 mOsmol/kg efficiently activated the GFP reporter in multiple cell types, including neuronal and gut stem cells, dendritic cells, embryonic fibroblasts, glia cells, and neurons (Figure 3E). The above experiments demonstrate a highly efficient protein transduction method that is applicable to many primary cell types.

We also explored whether human embryonic stem cells (hESCs) could be transduced using this method. We used H1 hESCs stably transduced with a lentiviral Cre-activatable reporter containing an active red fluorescence protein (RFP) gene flanked with LoxP sites, followed by a stop sequence and a (inactive) GFP reporter gene (Figure 3F). Cre-mediated deletion of the loxP-flanked RFP-stop segment activates the GFP reporter. The H1 reporter hESC line was transduced with Cre protein for 12 hr at 500 mOsmol/kg. As shown in Figure 3G, we obtained 64% and 78% of GFP-positive cells after one and two rounds of Cre protein transduction, respectively.

(E) MEFs were transduced with 1 μM of beta-lactamase protein, 25 mM NDSB-201 at different NaCl-adjusted osmolalities (indicated by the color lines) and for varying amounts of time as indicated. Isotonic media (open rhombs) containing NSDB-201 and beta-lactamase protein, but without additional NaCl, were used as a negative control. Relative beta-lactamase activity calculated per well is plotted as a function of transduction time. Dotted lines indicate the presence of cell death due to prolonged transduction conditions. Mean ± SD, n = 4.

(F) Analysis of the transduction activity of different hypertonicity inducers. MEFs were transduced for 3 hr with 1 μM beta-lactamase protein at an osmolality of 700 mOsmol/kg induced by different compounds as indicated (red bars, transduction with NDSB-201; open circles, control transduction in the absence of NDSB-201). Relative beta-lactamase protein uptake in isotonic transduction media (bar #1) was set at 1. Mean ± SD; n = 3.

(G) Beta-lactamase reporter assay on MEFs transduced for 3 hr with 1 μM of beta-lactamase protein with different concentrations of NDSB-201 with an osmolality of 700 mOsmol/kg induced by NaCl (red bars). The controls were cells treated as before but with isotonic media (white circles). Mean ± SD; n = 3.

(H) Beta-lactamase reporter assay on MEFs transduced as in (G) with different concentrations of beta-lactamase protein (red bars). The controls were cells treated as before in isotonic media (white circles). Mean ± SD; n = 3.

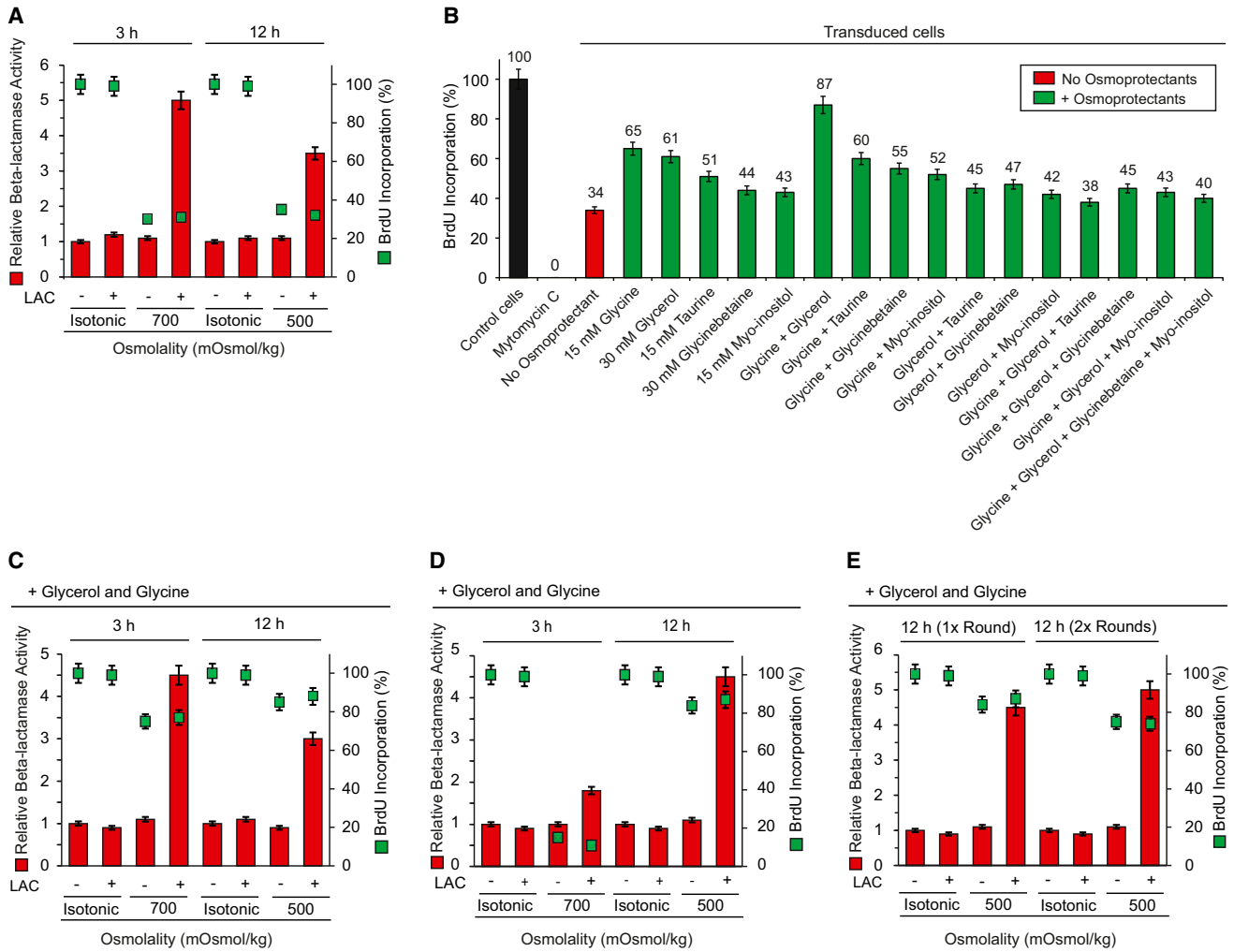

Figure 2. Addition of Osmoprotectants to the Transduction Media Ameliorates Hypertonicity-Induced Cell-Cycle Inhibition

(A) Beta-lactamase assay (red bars) coupled with BrdU incorporation assay (green squares). MEFs were transduced with 25 mM NDSB-201 at different osmolalities and time points with or without beta-lactamase as indicated. Beta-lactamase activity was measured relative to cells incubated in isotonic media, which were set at 1. Cell proliferation was measured by BrdU incorporation as described in the methods. BrdU incorporation of untreated cells was set at 100% (not shown). Mean ± SD; n = 3.

(B) MEFs were incubated with transduction media, containing 1 μM of beta-lactamase protein, 50 mM of NDSB-201, and an osmolality induced by NaCl of 500 mOsmol/kg (red bar) or with transduction media supplemented with different osmoprotectants as indicated (green bars). The BrdU incorporation values of untreated cells (left black bar) were set at 100%. BrdU incorporation values of mitomycin-C-treated cells used as control for cell-cycle arrest were set at 0%. Mean ± SD; n = 3.

(C) Beta-lactamase transduction (red bars) and BrdU incorporation (green squares) in MEFs. Cells were transduced with 25 mM NDSB-201 at different osmolalities and time points with or without Beta-lactamase as indicated with addiction of 30 mM of glycerol and 15 mM of glycine as osmoprotectants. Beta-lactamase activity was measured relative to cells incubated in isotonic media, which were set at 1. The BrdU incorporation values of untreated cells and mytomycin-C-treated cells were set at 100% and 0%, respectively (not shown). Mean ± SD; n = 3.

(D) Beta-lactamase transduction (red bars) and BrdU incorporation (green squares) in mESCs as in (C). Mean ± SD; n = 3.

(E) Beta-lactamase transduction (red bars) and BrdU incorporation (green squares) in mESCs after one or two rounds of protein transduction. mESCs were transduced once or twice as indicated with a 12 hr interval between transductions. The relative beta-lactamase activity was measured in relation to cells incubated in isotonic media, which were set at 1. The BrdU incorporation values of untreated cells and mytomycin C treated cells were set at 100% and 0%, respectively (not shown). Mean ± SD; n = 3.

Essential Structural Features of the Transduction Compound

As shown, the small-molecule NDSB-201 is essential for the introduction of native protein into cells. NDSB-201 is part of a group of zwitterionic compounds used to reduce protein aggregation and facilitate protein refolding (Vuillard et al., 1995). Six different NDSB molecules are commercially available (Figure 4A). To determine the essential chemical properties of NDSB-201,

we analyzed the transduction activity of these NDSBs and their effect on cell survival. As described before, MEFs were transduced with beta-lactamase protein for 3 hr with NaCl-adjusted osmolality of 700 mOsmol/kg. Beta-lactamase protein transduction of NDSB-201 (reference molecule #01) was set as 100%. As shown in Figure 4A, all NDSB molecules were capable of transducing beta-lactamase protein but with varying efficiencies and impact on cell proliferation. Whereas molecules #02 and #03 performed similar or better than our reference compound, molecules #04 and #06 lowered beta-lactamase transduction levels and reduced cell proliferation rate; molecule #05 performed poorly and arrested cell cycle, even in the presence of osmoprotectants.

It is well known that the sulfonate group is a potential cause of small-molecule toxicity. Thus, we replaced the sulfonate group in molecules #01 and #03 with a carboxyl group (generating molecules #09 and #10, Figure 4B) and tested the effect on transduction and cell proliferation. As shown in Figure 4B, replacement of the suphonate group did not affect protein transduction efficiency but further improved cell proliferation, reaching values of 95% of BrdU incorporation compared to non-transduced controls.

Further reducing the complexity of compound #09 yielded compound #11, in which the permanently positively charged quaternary amine group of compound #09 was replaced by a primary amine. The resulting molecule is gamma-amino-butyric acid (GABA), which exists as a zwitterion at neutral pH and thus contains a similar positive and negative charge at the molecule's termini. As shown in Figure 4B, GABA yielded excellent protein transduction efficiency and minimal effect on cell proliferation, with BrdU incorporation rate of 95% compared to untransduced controls. The finding that GABA, a well-known neurotransmitter, can mediate protein transduction was unexpected and suggested the involvement of GABA signaling in this process. However, protein transduction was not affected by neither the addition of well-known GABA agonists (Figure S2A) nor specific inhibitors of GABA receptor signaling (Figure S2B). Moreover, the concentration at which GABA is effective in protein transduction (25 mM) is similar to the concentration of NDSB-201 and is about 10,000-fold higher than its EC_{50} as a neurotransmitter (±2.5 μM; Mortensen et al., 2010). Therefore, it seemed likely that the physicochemical properties of GABA, rather than its role as a signaling molecule, were responsible for its protein-transducing activity. As mentioned above, the non-detergent sulfobetaine (NDSB) compounds were developed for their ability to enhance protein solubility (Vuillard et al., 1995). We therefore tested whether GABA could similarly prevent protein aggregation. A particularly insoluble protein is Cas9, an RNA-guided nuclease that can be used for specific gene editing, which we will describe in more detail below. Production and purification of recombinant Cas9 protein proved particularly challenging and required a higher concentration of NDSB-201 to prevent the protein aggregation and precipitation. To test whether GABA was similarly able to promote protein solubility, we made a dilution series of either NDSB-201 or GABA and added recombinant Cas9 protein at a final concentration of 10 μM. NDSB-201 efficiently prevented protein precipitation at a concentration of 200 mM. As shown, GABA could substitute NDSB-201 and prevent protein aggregation at similar concentrations (Figure 4C).

At neutral pH, NDSBs and its analogs (Figure 4) are zwitterionic compounds that have a negatively charged hydrophilic group, a short 3-carbon hydrophobic chain and a positively charged amine terminus with various possible substituents. The hydrophobic middle domain is too short to form micelles, and thus, NDSBs are not considered detergents (Vuillard et al., 1995). To identify the minimal essential structure necessary for transduction, we tested the beta-lactamase protein transduction activity of several analogs of NDSB and/or GABA (Figure 4D). We analyzed the importance of the charged amine and sulfonate/carboxyl termini of the molecules by removing these groups from the structure. The analogs lacking the amine (#07 and #12, Figure 4D) or the sulfonate/carboxyl groups (#08 and #13, Figure 4D) yielded very poor protein transduction levels and reduced cell proliferation, although cell survival and beta-lactamase protein solubility were not affected (data not shown). These data demonstrate that the presence of the amine and sulfonate/carboxyl groups at the transduction compound termini is essential for protein transduction. Finally, we evaluated the optimal distance between the amine and sulfonate/carboxyl groups by varying the length of the carbon chain in molecules #10 and #11 (Figure 4E). As shown in Figure 4E, a deleterious effect on protein transduction was observed when the carbon chain was shorter or longer than three carbons. Above data demonstrate that the minimal structure necessary to allow efficient protein transduction is a zwitterionic molecule, which, at neutral pH, consists of a positively charged amino group and a negatively charged sulfonyl or carboxyl group separated by a three-carbon chain. To assure that the reduced transduction efficiencies observed by some of the compounds were not the result of poor protein solubility, we analyzed beta-lactamase protein precipitation in the presence of different betaine compounds. With the exception of the control sample, in which protein precipitation was induced by adding ethanol, the different transduction compounds mentioned above did not induce beta-lactamase protein precipitation (Figure S2C).

Dissecting the Mechanism of Protein Transduction

Because proteins are too large to diffuse through the plasma membrane, we suspected that protein transduction involved an active transport mechanism. Extracellular particles can enter via several distinct endocytic pathways: dynamin-dependent endocytosis, which is further subdivided in clathrin- and caveolae-mediated endocytosis, and dynamin-independent endocytosis, which includes macropinocytosis, the uptake of large (0.5–5 μm) vesicles containing gulps of extracellular fluid. We used specific inhibitors of these endocytic pathways to determine the mechanism of protein uptake. MEFs were incubated with inhibitors of dynamin-, clathrin-, or caveolin-mediated endocytosis or macropinocytosis for 1 hr prior to transduction with beta-lactamase protein. As shown in Figure 5A, inhibition of dynamin-, clathrin-, or caveolin-mediated endocytosis did not affect beta-lactamase uptake. In contrast, the macropinocytosis inhibitors 5-(N-Ethyl-N-isopropyl)amiloride (EIPA) and 5-(*N*,*N*-Dimethyl)amiloride (DMA) resulted in a profound reduction in beta-lactamase transduction. Macropinocytosis requires

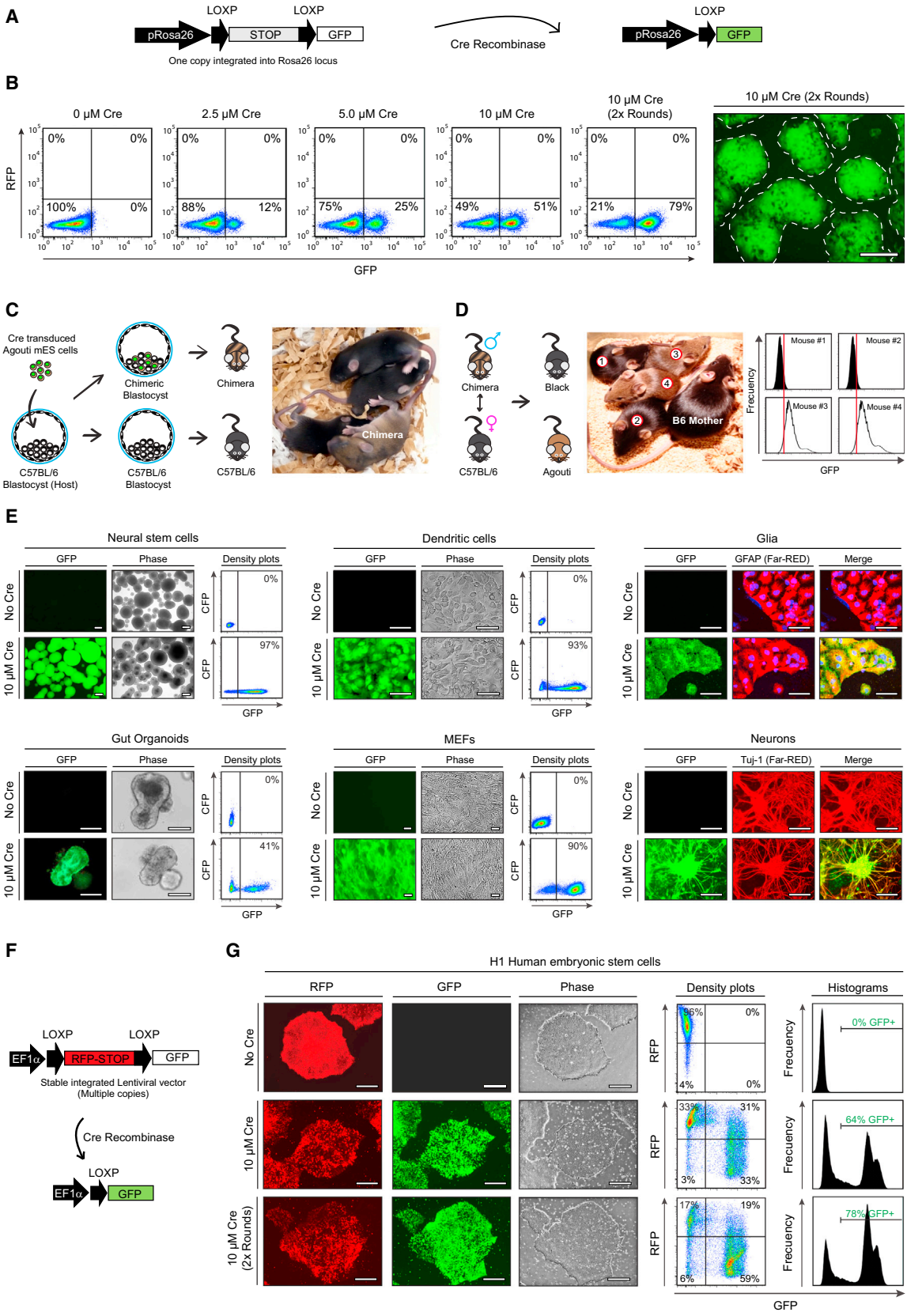

(legend on next page)

active rearrangements of the actin cytoskeleton, which is mediated by the small GTPases Rac1 and CDC42 through activation of the downstream effector kinase Pak1. As expected, cytochalasin D or latrunculin A, which potently block actin polymerization, inhibited beta-lactamase transduction (Figure 5A). In addition, specific inhibitors of RAC1, CDC42, and Pak1 alone or in combination efficiently block beta-lactamase transduction in MEFs (Figures S3A and S3B). Altogether, these results indicate that protein transduction is mediated through macropinocytosis.

Macropinocytosis is regulated by a family of Na^+/H^+ antiporters, which are targeted by the EIPA and DMA inhibitors described above. These NHE antiporters are rapidly activated in response to a wide variety of extracellular stimuli, including hypertonicity induced by Na^+-containing salts. Nhe1 (Slc9A1) is a ubiquitously expressed member of this family and therefore is a likely candidate to be involved in the protein transduction process. To determine the role of Nhe1 in protein transduction, we analyzed beta-lactamase protein transduction in Nhe1 mutant MEFs. Heterozygous or homozygous deletion of Nhe1 resulted in a profound reduction in intracellular beta-lactamase activity, demonstrating that Nhe1 plays an important role in protein transduction (Figure 5B). The residual protein transduction activity observed in the absence of Nhe1 function is likely a redundant effect of other members of the Nhe antiporter family.

Several growth factor activators of tyrosine kinase signaling were shown to stimulate macropinocytosis. Therefore, we examined whether the addition of growth factors could enhance intracellular delivery of beta-lactamase protein. As shown in Figure 5C, EGF, bFGF, PDGF, IGF, and insulin all enhanced beta-lactamase transduction, and combinations demonstrated an additive effect.

The above data demonstrate that iTOP protein transduction occurs through macropinocytosis uptake of extracellularly applied protein, which is subsequently released from the internalized macropinosomes. To quantify the differential roles of NaCl hypertonicity and the transduction compound in protein uptake and intracellular release, we set up two imaging-based assays.

Macropinocytosis can be quantified by measuring the uptake of fluorescently labeled high-molecular-weight dextran (Figure 5D; Commisso et al., 2014). To determine whether dextran carbohydrate uptake and protein uptake followed the same path, MEFs were co-transduced with red fluorescent dextran (TMR-dextran) and far-red fluorescent BSA protein (BSA-Alexa647) for 1 hr at 700 mOsmol/kg. As shown in Figure 5D, all dextran-positive macropinosomes contained BSA and vice-versa, demonstrating that the uptake of TMR-dextran and proteins proceed via the same mechanism (Figure 5D). Moreover, the simultaneous uptake of Dextran and BSA was blocked by the macropinocytosis inhibitor EIPA (Figure 5D). Together, these data demonstrate that the recently described TMR-dextran assay for the quantification of macropinocytosis (Commisso et al., 2014) can be utilized to accurately monitor the macropinocytotic uptake step in the iTOP process.

To quantify the release of internalized macropinosomes, we used a galectin3-fluorescent reporter system that has been described earlier to monitor vesicle leakage induced by drugs or pathogens (Paz et al., 2010; Ray et al., 2010). Galectin-3 is a small soluble cytosolic protein that can bind betagalactoside sugar-containing carbohydrates. These are normally present only on the exterior of the plasma membrane and the interior of intracellular endocytic vesicles. Rupture of internalized vesicles results in galectin-3 relocalization and accumulation at the internal vesicle membrane. Fusion of galectin-3 to a monomeric green fluorescent protein (mAG-GAL3) allows visualization of galectin-3 relocalization and has been used as a tool to monitor vesicle rupture during pathogen infection (Paz et al., 2010; Ray

Figure 3. Efficient Cre Protein Transduction in Multiple Primary Stem and Differentiated Cells

(A) Schematic representation of the Cre reporter in mESCs. A single copy of a loxP-Stop-loxP-GFP reporter was inserted in the Rosa26 locus. Excision of the Stop cassette by Cre-recombinase protein induces GFP expression.

(B) Left: FACS analysis of a dose response curve of mESCs transduced with Cre at different concentrations as indicated (panels 1–4) or after two rounds of Cre transduction (panel 5). Right: fluorescence microscopy image of mESCs treated with two rounds of Cre transductions as described above. Dashed lines indicate the border of each colony. Scale bar, 50 μm.

(C) Left: schematic representation of the mouse chimera assay. mESCs were injected into host blastocyst embryos, and mESC contribution to resulting chimeras is assessed by coat color. Cre-protein transduced GFP-positive mESCs derived from agouti (F1BL6/129Sv) mice (brown hair color) were injected into C57BL/6 host blastocyst (black hear color). Brown hair in the resultant pups indicates chimera contribution of the injected ESCs. Right: image of litter with chimera.

(D) Left: schematic representation of the germline transmission assay. Chimera in C was mated with a C57BL/6 female. Agouti coat color of resultant pups demonstrates the ESC origin of the germ cells. Center: image of litter with two agouti pups demonstrating germline transmission of the injected ESCs. Right: FACS analysis of GFP expression in blood cells of the pups depicted in the central panel. The agouti pups (#3 and #4) display GFP expression, whereas the black pups (#1 and #2) are negative.

(E) Left and middle: Cre protein transduction of multiple cells types derived from loxP-mRFP-loxP-mGFP reporter mice. Representative fluorescence and phase contrast images of Cre transduced cells. The control was cells incubated with transduction media without Cre protein. Scale bar, 50 μm. Percentage of GFP-positive cells was determined by flow cytometry. Right top: fluorescence microscopy images of Cre transduced glia cells. As control, cells were incubated with transduction media without Cre protein. Left: GFP expression. Middle: expression of GFAP, a glia-specific marker. Right: merge. Scale bar, 50 μm. Right bottom: fluorescence microscopy images of Cre transduced neural cells derived from loxP-stop-loxP-GFP mESCs. As control, cells were incubated with transduction media without Cre protein. Left: GFP expression. Middle: expression of TuJ1, a neural cell-specific marker. Right: merge. Scale bar, 50 μm.

(F) Schematic representation of the Cre recombinase reporter. A lentiviral EF1a-loxP-RFP-loxP-GFP/ires-PuroR construct was stably introduced into hESCs. Cre excises the loxP-flanked RFP-STOP cassette and switches fluorescence from red (RFP) to green (GFP).

(G) Left: fluorescence and phase contrast images of Cre-transduced human ESCs. hESCs were transduced once or twice with Cre protein as indicated. Control was cells incubated with transduction media without Cre protein. Left row, RFP expression; middle row, GFP expression; right row, phase contrast. Scale bar, 50 μm. Right: flow cytometry analysis of Cre-transduced human ESCs. The density plots show the percentage of cells expressing RFP (upper left area) or GFP (lower right area). Double-positive cells (upper right area) result from multiple integrations of the lentiviral reporter. Total percentage GFP expressing cells is shown in the histogram plots.

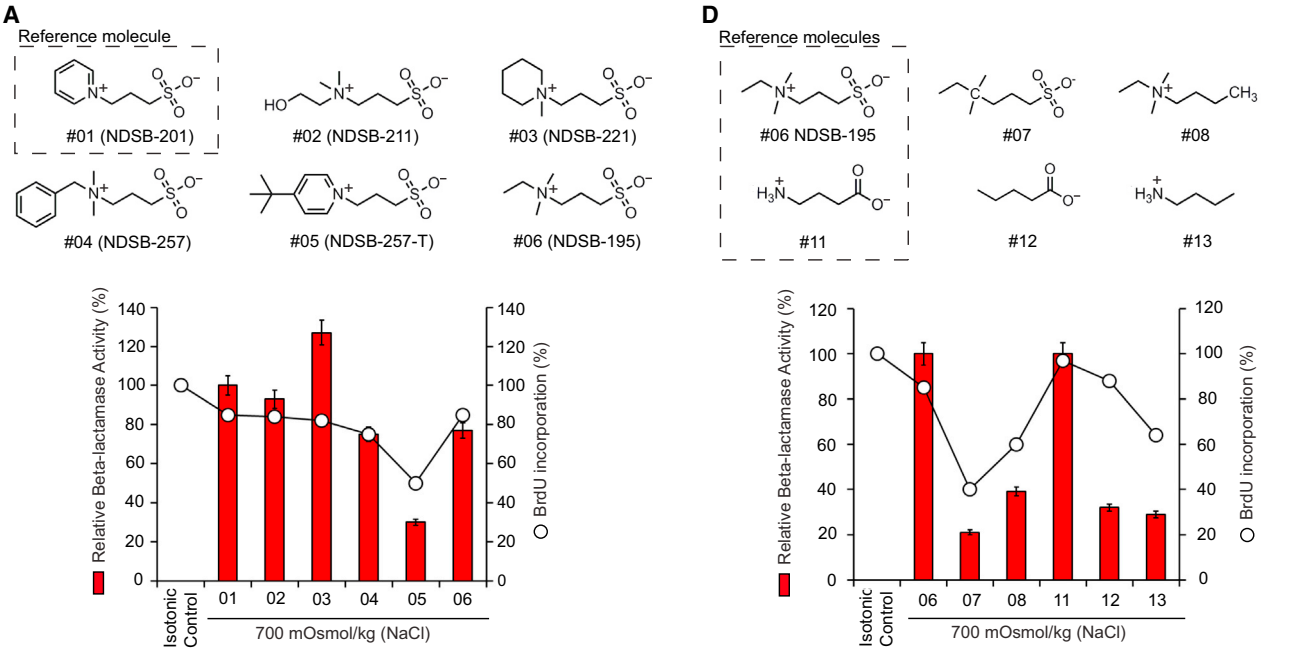

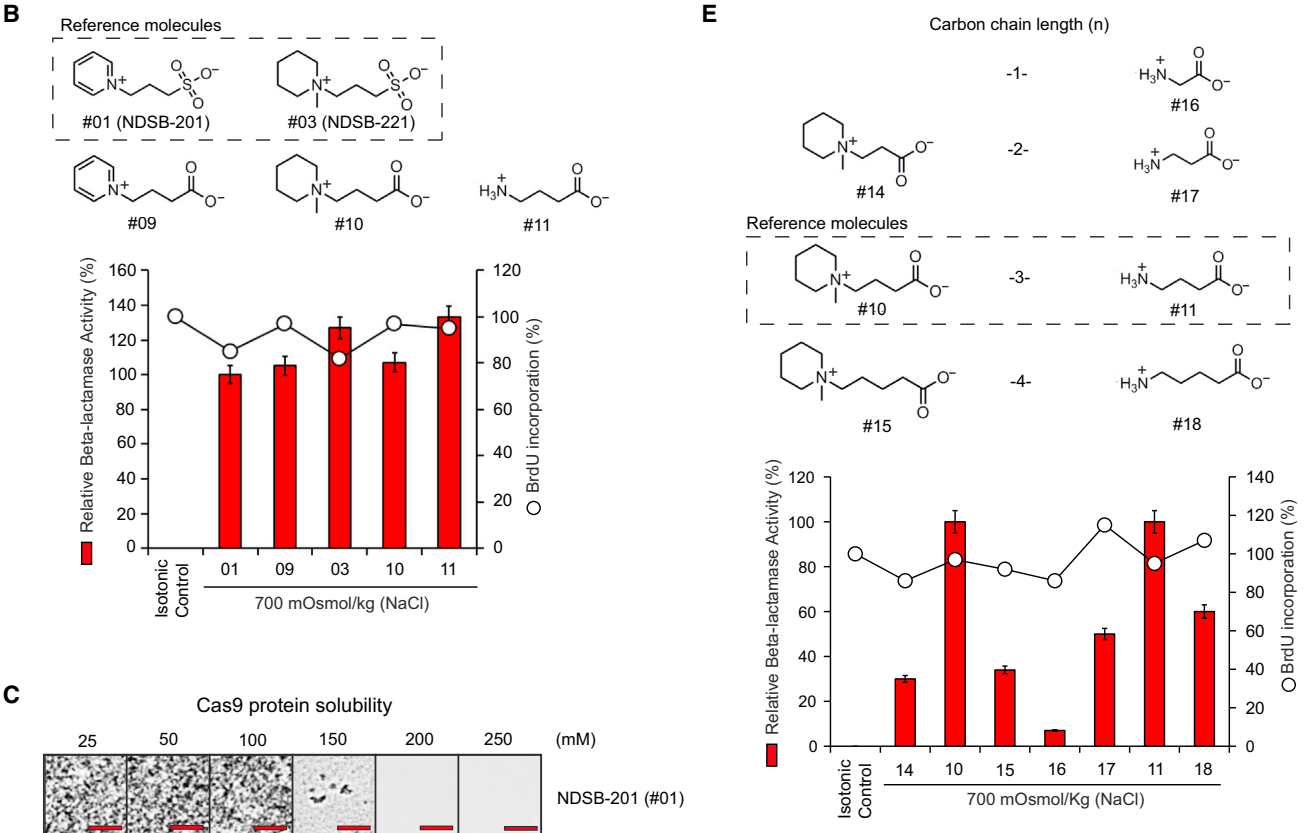

(legend on next page)

et al., 2010). Upon mAG-GAL3 binding to carbohydrates in the interior of ruptured vesicles, a multimer complex is formed with intense green fluorescence (Figure 5E). Transduction of MEFs expressing mAG-GAL3 protein for 1–3 hr at 700 mOsmol/kg resulted in the appearance of bright green vesicles, demonstrating leakage of the internalized macropinosome membrane under iTOP conditions. mAG-GAL3 vesicles were not formed when cells were pre-incubated with macropinocytosis inhibitor EIPA or under isotonic conditions (Figure 5E). These results demonstrate that iTOP conditions promote protein uptake from the extracellular space via macropinocytosis and induce macropinosome vesicle leakage to release proteins into the cytosol.

Using the above assays to quantify uptake and release, we measured beta-lactamase protein transduction, macropinocytosis, and vesicle leakage (Figure 5F). As expected, protein transduction measured by beta-lactamase assay was only observed in cells treated with hypertonic media in the presence of either NDSB-201 or GABA transduction compounds (Figure 5F, blue bars). Control compounds with a shorter carbon chain, glycine, and glycine-betaine, did not mediate beta-lactamase transduction even though macropinocytosis was induced in all hypertonic conditions (Figure 5F, red bars), indicating that NaCl hypertonic media alone are sufficient to efficiently induce macropinocytosis. Transduction compound alone, in the absence of NaCl-mediated hypertonicity, did not induce macropinocytosis (data not shown). The combined data on beta-lactamase transduction and macropinocytosis suggested that the transduction compounds were responsible for the release of protein from the internalized macropinosomes. Indeed, the mAG-GAL3 reporter assay demonstrated that intracellular macropinosome leakage only occurred in the presence of NDSB-201 or GABA (Figure 5F, green bars). When macropinosome leakage occurred, the vesicle contents were completely released into the cytoplasm (data not shown). Images of the mAG-GAL3 assay on the various compounds used in Figure 5F are shown in Figure S3C. The macropinocytosis inhibitor EIPA efficiently blocked both beta-lactamase protein transduction, macropinocytosis, and the appearance of mAG-GAL3-positive vesicles. Together, these data indicate that NaCl hypertonicity induces macropinocytosis-mediated uptake of protein from the extracellular space, whereas NDSB-201 or GABA molecules promote intracellular macropinosome leakage, allowing the release of the vesicle content into the cytosol.

Protein-Mediated Gene Editing

The high efficiency of iTOP has appealing application in systems in which transient cell manipulation can elicit a binary cellular effect or response. The recently discovered CRISPR-Cas9 system consists of the Streptococcus Pyogenes Cas9 nuclease protein, which is guided to specific genomic loci by a small guide RNA (sgRNA) (Charpentier and Doudna, 2013). The Cas9 nuclease creates a double-strand break at the target locus, which, when repaired through non-homologous end joining (NHEJ), frequently results in gene disruption by the resulting frame shift mutation. Due to its elegant simplicity, the CRISPR-Cas9 system has quickly become a popular tool for gene editing. However, application of this system by means of DNA or RNA transfection is inefficient in primary cells and typically requires marker selection of transfected cells. We explored whether iTOP of recombinant Cas9 protein and its guide RNA can offer an alternative, more efficient means of applying this gene-editing system.

As shown above, Cas9 protein requires high concentrations of both salt (500 mM NaCl) and the transduction compound (250 mM) to remain soluble (Figures 4C and S4A). We noticed that, under this condition, the NSDB-201 transduction compound was toxic to the cells, but GABA was well tolerated (Figures S4B and S4C). At this tonicity (1,250 mOsm/Kg),

Figure 4. Structure-Activity Analysis of Protein Transduction Compounds

(A) Top: chemical structures of tested non-detergent sulfobetaines. Compound numbers are indicated below the structure. Bottom: beta-lactamase and BrdU incorporation assays using the different transduction compounds as indicated. MEFs were transduced for 3 hr with transduction media containing a NaCl-adjusted osmolality of 700 mOsmol/kg, 1 μM Beta-lactamase protein, 30 mM of Glycerol, 15 mM of Glycine, and 25 mM of the indicated transduction compounds. Beta-lactamase incorporation values of cells treated with transduction media with the reference compound (NDSB-201, #01) were set as 100%, and values of cells treated with isotonic transduction media were set as 0%, as described in the Experimental Procedures. Open circles indicate relative BrdU incorporation by the transduced cells. BrdU incorporation of untransduced cells was set at 100%, and BrdU incorporation of mitomycin-C-treated cells was set at 0%. Mean ± SD; n = 3.

(B) Top: chemical structures transduction compound analogs. First row: tested analogs with sulfonic group. Second row: analogs with carboxy group. Compound numbers are indicated below the structure. Bottom: beta-lactamase and BrdU incorporation assays using the different transduction compounds as indicated. MEFs were transduced as described in (A). Beta-lactamase activity and BrdU incorporation values were analyzed as in (A). Mean ± SD; n = 3.

(C) Images demonstrating the effect of increasing concentrations of the transduction compounds NSDB-201 or GABA on Cas9 protein solubility. From left to right, increasing transduction compound concentration (mM). Rows are different transduction compounds. Scale bar, 50 μm.

(D) Top: chemical structures of transduction compounds analogs. Compounds in left columns contain amine and sulfonate or carboxy group. Central column shows analogs without amine group. Right column shows analogs without sulfonate or carboxy group. Compound numbers are indicated below the structure. Bottom: beta-lactamase and BrdU incorporation assays using the different transduction compounds as indicated. MEFs were transduced with beta-lactamase protein and beta-lactamase activity and BrdU incorporation were analyzed as in (A). Beta-lactamase activity of the reference compounds (NDSB195, #06 and GABA, #11) was set at 100%. Values derived from compounds #07 and #08 were referred to compound #6. Values derived from compounds #12 and #13 were referred to compound #11. Beta-lactamase activity of cells treated with isotonic transduction media was set as 0%. BrdU incorporation is shown as open circles as in (A). Mean ± SD; n = 3.

(E) Analysis of the role of the carbon-chain length. Structures are examples of two transduction compounds (reference molecules #10 and #11) with carbon-chain length variations of these. Bottom: beta-lactamase and BrdU incorporation assays using the different transduction compounds as indicated. MEFs were transduced with beta-lactamase protein, and beta-lactamase activity and BrdU incorporation were analyzed as in (A). Beta-lactamase incorporation of the reference compounds (#10 and #11) was set at 100%. Beta-lactamase activity of cells treated with isotonic transduction media was set as 0%. Values derived of compound #14 and #15 were referred to compound #10. Values derived of compound #16, #17, and #18 were referred to compound #11. BrdU incorporation is shown as open circles as in (A). Mean ± SD; n = 3. For more details of the transduction compounds and their analogs, see Table S2.

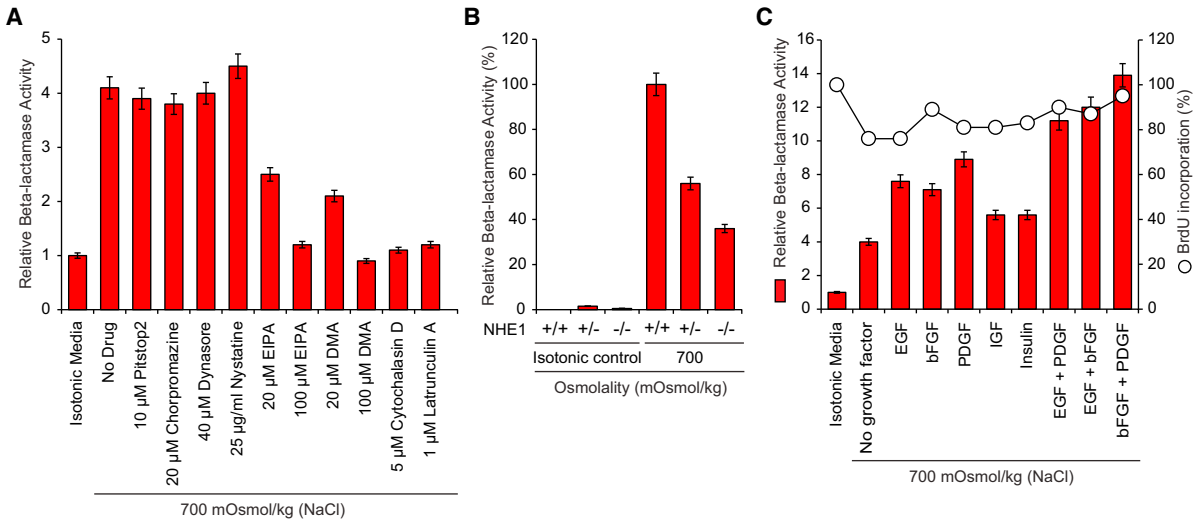

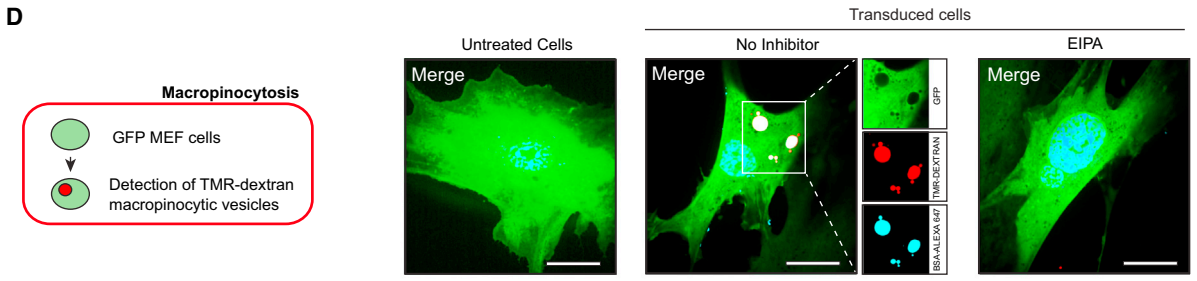

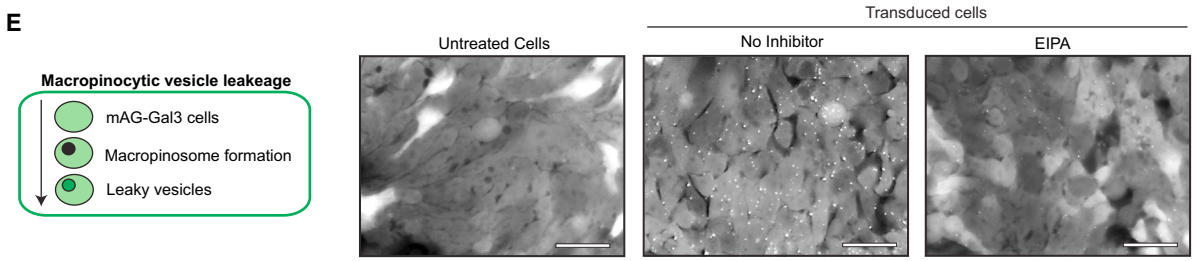

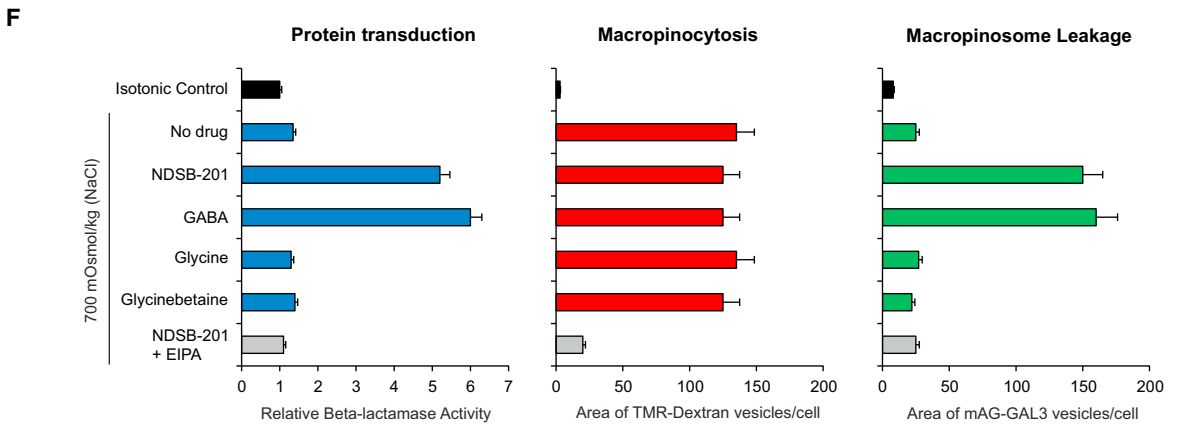

(legend on next page)

transduction occurs within 60–90 min and is extremely efficient, as shown by the transduction of recombinant Cre protein (Figures S4D–S4F). Previous reports have demonstrated that hypertonic stress can cause DNA breaks in inactive regions of the genome (Redon and Bonner, 2011). However, our iTOP transduction conditions include osmoprotectants, which should prevent DNA damage from occurring. We performed a TUNEL (terminal deoxynucleotyl transferase dUTP nick end labeling) assay to determine the effect of our iTOP hypertonic conditions in the presence or absence of osmoprotectants. As expected, the osmoprotectants in the iTOP transduction buffer effectively prevented hypertonicity-induced DNA damage (Figure S4G). In addition to the recombinant Cas9 protein, CRISPR/Cas9 gene editing requires intracellular delivery of sgRNAs. To determine whether iTOP transduction allows the intracellular delivery of RNA molecules as well, we analyzed the effect of siRNA transduction in knocking down target GAPDH. As shown in Figure S4H, iTOP transduction of siRNA resulted in efficient and specific knockdown of target GAPDH, demonstrating that, in addition to protein, iTOP transduction can be used for the delivery of small RNAs as well.

To explore whether recombinant Cas9 protein and guide RNA could be co-transduced into cells under iTOP conditions (iTOP-CRISPR/Cas9), we produced recombinant Cas9 protein and generated sgRNAs by in vitro transcription from DNA templates (Figure 6A). A reporter in which the presence of an AAVS1 target sequence produces an out-of-frame non-fluorescent dTomato gene was used to monitor the introduction of recombinant Cas9-sgRNA (Figure 6B). CRISPR-Cas9 targeting of the AAVS1 sequence results in a frame shift and activates dTomato fluorescence. KBM7 cells stably expressing the reporter were transduced with Cas9 protein together with the corresponding AAVS1 sgRNA. After one round of Cas9-sgRNA transduction, 30% of reporter KBM7 cells reestablished dTomato protein expression (Figure 6C). Upon a second round of Cas9-sgRNA transduction, 56% of the cells became dTomato positive. Targeting was specific to the AAVS1 sequence because off-target sgRNAs with two nucleotide substitutions did not activate the dTomato reporter (Figure 6C). Similar experiments were performed in H1 human embryonic stem cells with an observed efficiency of 10% and 26% of dTomato-positive cells after one and two rounds of transduction, respectively (Figure 6D). The above results demonstrate that iTOP of recombinant Cas9 protein and sgRNA allows efficient and specific gene modification in reporter cells.

To determine the efficiency of the iTOP-CRISPR/Cas9 system, we targeted an endogenous gene. We chose to target *DPH7* (WDR85), a gene that was identified as an essential host factor for Diphtheria toxin lethality (Carette et al., 2009). Biallelic deletion of *DPH7* renders human cells resistant to Diphtheria toxin-induced cell death, providing a simple and effective means of identifying knockout cells and measuring the efficiency of biallelic gene knockout upon iTOP-CRISPR/Cas9. We used a near-diploid clone of the KBM7 cells to disrupt the *DPH7* gene (Figure S5A). KBM7 cells were transduced twice with Cas9 protein, plus one of six different sgRNAs as are indicated in Figure 7A. Seven days after protein transduction, cells were treated with diphtheria toxin for 48 hr, after which the number of viable

Figure 5. Protein Transduction Is Mediated by Macropinocytosis

(A) MEFs were preincubated for 1 hr and transduced for 3 hr in the presence of small-molecule inhibitors of dynamin-mediated endocytosis (Dynasore), Clathrin-mediated endocytosis (Pitstop2 and chlorpromazine), Caveolin-mediated endocytosis (Nystatin), macropinocytosis (EIPA, Ethylisopropylamiloride and DMA, Dimethylamiloride), or actin polymerization (Cytochalasin D and Latrunculin A) as indicated. MEFs were transduced for 3 hr with 1 μM beta-lactamase protein at a NaCl-adjusted osmolality of 700 mOsmol/kg in transduction media containing 25 mM of NDSB-201, 30 mM of Glycerol, and 15 mM of Glycine supplemented with small-molecule inhibitors as indicated. Relative beta-lactamase protein uptake in isotonic transduction media (left bar) was set at 1. Mean ± SD; n = 3.

(B) Role of Nhe1 in protein transduction. MEFs derived from wild-type, Nhe1 heterozygous ($^{+/-}$), and Nhe1 knockout ($^{-/-}$) embryos were transduced for 3 hr with 1 μM beta-lactamase as in (A). Beta-lactamase transduction values of wild-type cells (bar #4) were set at 100%, and beta-lactamase transduction of wild-type cells in isotonic media (Bar #1) was set at 0%. Mean ± SD; n = 3.

(C) The effect of growth factors on beta-lactamase transduction. MEFs were transduced for 3 hr with 1 μM beta-lactamase protein at a NaCl-adjusted osmolality of 700 mOsmol/kg as in (A) in the presence of 20 ng/ml of epidermal growth factor (EGF), 20 ng/ml of basic fibroblast growth factor (FGF), 20 ng/ml of platelet-derived growth factor (PDGF), 20 ng/ml of insulin growth factor (IGF), 2.5 μg/ml of insulin, and combinations of growth factors as indicated. Beta-lactamase values of cells in transduction media without growth factor (bar #2) were set at 100%, and beta-lactamase values of cells in isotonic transduction media (bar #1) were set at 0%. Open circles indicate relative BrdU incorporation by the transduced cells. BrdU incorporation of untransduced cells was set at 100%, and BrdU incorporation of mitomycin-C-treated cells was set at 0%. Mean ± SD; n = 3.

(D) Left: schematic representation of the macropinocytosis quantification. Right: to assess whether the transduction buffer would permit the simultaneous incorporation of proteins and non-protein molecules, we analyzed macropinocytosis-mediated uptake of TMR dextran (red) and fluorescently labeled BSA protein (cyan) by GFP-expressing MEFs. Merge of red and cyan gives white by additive color mixture. Transduced cells were incubated at 700 mOsmol/kg with 25 mM NDSB-201. The macropinocytosis inhibitor, EIPA (ethylisopropylamiloride), inhibits uptake of TMR dextran and BSA protein. Nuclei were stained with Hoecht 33342 (blue). Scale bar, 50 μm.

(E) Left: schematic representation of the mAG-GAL3 reporter assay. Upon initiation of transduction, extracellularly applied protein is taken up into macropinosomes (black vesicles). Intracellular disruption of the macropinosome membrane releases the macropinosome content into the cytoplasm and allows entry of cytosolic mAG-GAL3 protein, resulting in a bright fluorescent signal (bright green vesicles). Right: mAG-GAL3 cells were incubated with transduction media at 700 mOsmol/kg supplemented with 25 mM NDSB-201 with or without the macropinocytosis inhibitor EIPA as indicated. Untreated cells were included as negative control. Note that, under transducing conditions (middle), mAG-GAL3 accumulates in the compromised macropinosomes. Scale bar, 200 μm.

(F) Measurement of protein transduction activity, macropinocytosis, and macropinosome vesicle leakage of NDSB-201 and examples of derivative compounds. Cells were incubated with transduction buffer at 700 mOsmol/kg with different transduction compounds or left untreated, as indicated. Left: relative beta-lactamase protein incorporation in MEFs. Beta-lactamase transduction of cells in isotonic transduction media (black bar) was set at 1. Middle: macropinocytosis levels were measured by TMR dextran incorporation in cells treated as described above, and total area of dextran positive vesicles per cell was determined. Right: macropinosome leakage was determined by measuring total area of mAG-Gal3-positive vesicles per cell. Mean ± SD; n = 3.

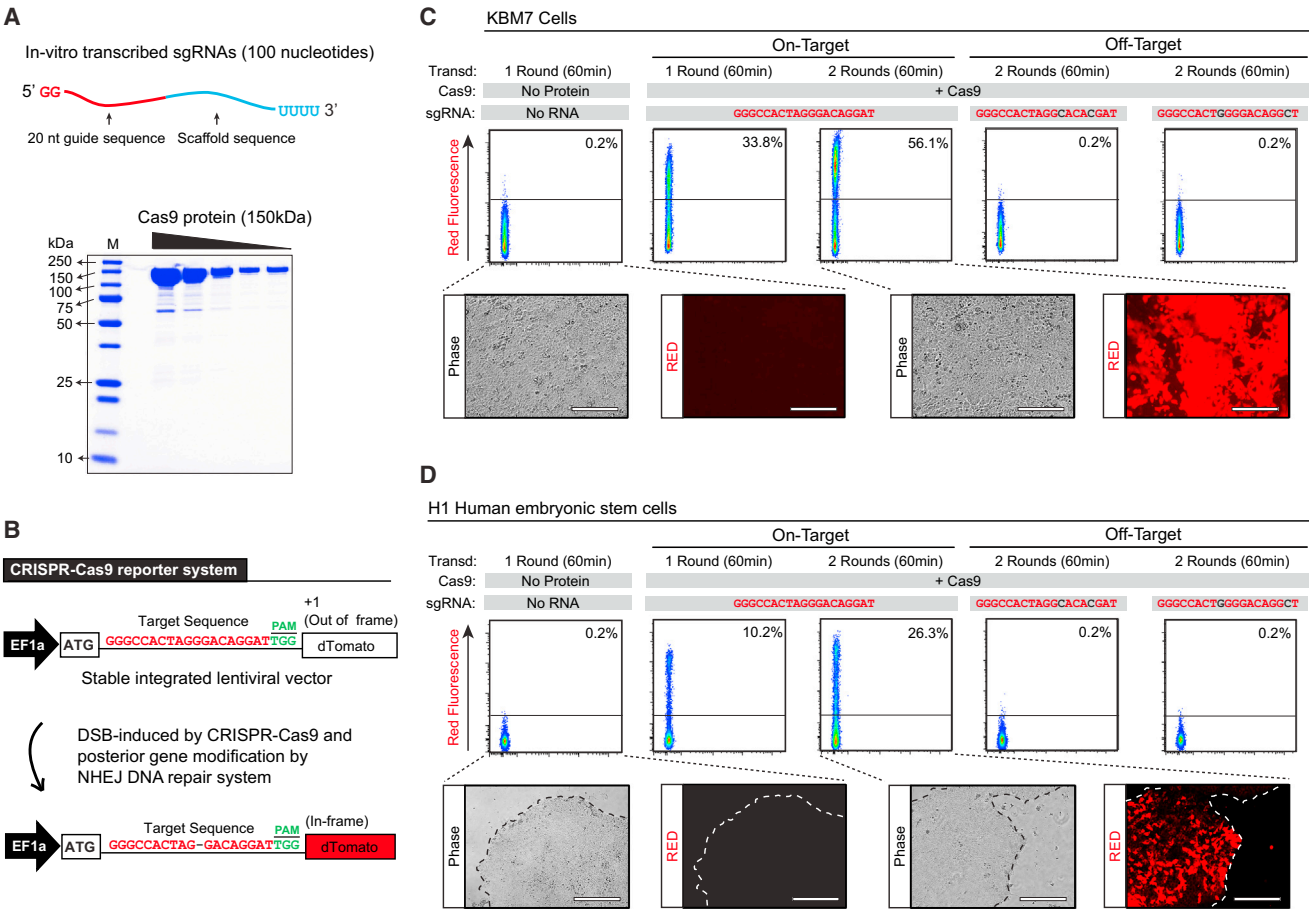

Figure 6. Gene Editing Using Simultaneous Transduction of Recombinant Cas9 Protein and sgRNA

(A) Top: schematic representation of the in-vitro-transcribed sgRNAs containing 20 nucleotides of guide sequence and 80 nucleotides of scaffold sequence. Bottom: protein gel of recombinant purified Streptococcus pyogenes Cas9 protein.

(B) Schematic representation of the CRISPR-Cas9 reporter system. Cells were transduced with a lentiviral vector containing the CRISPR-Cas9 target sequence followed by an out-of-frame sequence of dTomato gene. CRISPR-Cas9 induced DNA double-strand break in the target sequence, followed by NHEJ repair that induces DNA deletions and/or insertions. Those DNA modifications may restore the dTomato reading frame, producing red cellular fluorescence. DNA sequences in red and green represent the "target sequence," where red and green text represents the "sgRNA binding" sequence and the "protospacer-adjacent motif, PAM" sequence, respectively.

(C) CRISPR-Cas9 reporter KBM7 cells were transduced with Cas9 protein and target sgRNA. Negative control was cells transduced without Cas9 and sgRNA. Specificity controls were performed by transducing cells with Cas9 protein and off-target sgRNAs. The percentage of dTomato-positive cells was determined by flow cytometry analysis. Bottom shows phase contrast and fluorescent images for indicated conditions. Scale bar, 250 μm.

(D) CRISPR-Cas9 reporter H1 human embryonic stem cells were transduced with Cas9 protein and on-target sgRNA. Negative control was cells transduced without Cas9 and sgRNA. Specificity controls were performed by transducing cells with Cas9 protein and off-target sgRNAs. The percentage of dTomato-positive cells was determined by flow cytometry analysis. Bottom shows phase contrast and fluorescent images for indicated conditions. Dotted lines delineate the border of the hES colony. White scale line represents 50 μm.

cells was determined. Samples transduced with Cas9 protein and *DPH7* sgRNAs yielded high levels of cell survival, whereas no viable cells were detected in diphtheria-toxin-treated wild-type KBM7 cells or in cells transduced with Cas9 protein with a control sgRNA (Figure 7A). DNA sequence analysis on the pool of diphtheria-toxin-resistant cells demonstrated *DPH7* gene disruption at the sgRNA target site in all resistant cells (Figures 7B and S5B), confirming that diphtheria toxin resistance was the result of Cas9-sgRNA targeting. Similar results were obtained when H1 human ESCs were targeted with recombinant Cas9 protein coupled to *DPH7* sgRNAs (Figure 7C).

To determine the frequency of biallelic *DPH7* gene disruption, we transduced KBM7 and H1 cells with Cas9 protein and the corresponding *DPH7* sgRNA as described above. Upon transduction, single cells were sorted into 384-well plates (Figure 7D). After a week, emerging clones were treated with diphtheria toxin, and resistant clones were counted to quantify the percentage of knockout clones. Four out of six sgRNAs yielded around 70% resistant clones, which is a remarkable efficiency considering that diphtheria resistance requires biallelic deletion of *DPH7* gene (Figure 7D). Indeed, sequence analysis revealed biallelic mutations at the sgRNA target sites in all clones analyzed

(Figure 7E, top). Similar results and knockout efficiency were obtained upon transduction of human ESCs (Figure 7E, bottom). Above results demonstrate the particular strength of the iTOP-CRISPR/Cas9 system in enabling high-efficiency gene editing in primary (stem) cells (Figure S5C). *DPH7* knockout clones of hESCs retained expression of essential hESC markers, as well as the ability to generate derivatives of all three germ layers in vitro, demonstrating that iTOP-CRISPR/Cas9 gene knockout did not affect stem cell pluripotency (Figure S6).

Conclusions

Despite vast improvement in technologies for the delivery of DNA or RNA into cells, the manipulation of primary cells often remains difficult, with low percentages of targeted cells, poor control over insert copy number, and/or unstable gene expression levels. The ability to efficiently transduce native proteins into primary cells offers new opportunities for direct cell manipulation without the need for DNA or RNA intermediates. Proteins allow cell manipulation in a non-integrative manner and are particularly suited in binary systems in which a single, transient cell manipulation results in a permanent change in cell function, identity, or (epi)genetic state.

The iTOP system described here is highly efficient and flexibly adaptable. Variation in NaCl hypertonicity, type and concentration of transduction compound, and variation in transduction time can be fine-tuned to the needs of the user, the specific target cell type, and the biochemical characteristics of the transduced protein. Because the amount of transduced protein is directly related to the extracellular protein concentration, the system allows narrow dosage of the effective intracellular protein levels.

The CRISPR/Cas9 gene editing has revolutionized our ability to modulate the genome and development of a safe and efficient means to apply this technology in primary cells allowing the use of CRISPR/Cas9 in the modulation of genetic defects. Recent reports demonstrate that delivery of recombinant Cas9 protein using CPPs, electroporation, or cationic lipids results in effective gene editing of immortalized cell lines, but primary cells remain a challenge (Kim et al., 2014; Ramakrishna et al., 2014; Zuris et al., 2014). We demonstrate that the iTOP system allows highly efficient gene modification upon transduction of recombinant Cas9 protein and in-vitro-transcribed sgRNA (iTOP-CRISPR/Cas9). The transient nature of iTOP-CRISPR/Cas9 assures that the transduced gene-editing system does not remain inside the cell, leaving only the editing event as a permanent result of the cell manipulation. The high efficiency to knockout genes using protein iTOP has appealing application in research and perhaps will allow new therapeutic avenues for the treatment of genetic disease. In addition to gene editing, protein iTOP may have application in other areas, for example in the modulation of intracellular signaling pathways, in cell differentiation/dedifferentiation, or as adjuvants in dendritic cell immunization.

EXPERIMENTAL PROCEDURES

Cell Lines

COS7 cells—ATCC, H1 human ESCs—WiCell, and KBM7 cells were a gift from Dr. Brummelkamp, NKI Amsterdam. Mouse embryonic neural stem (NSC) cells were derived from E13.5 mice embryos as described by Louis and Reynolds (2005). Mouse gut organoids were derived from adult mice as reported by Sato et al. (2009).

Cell Proliferation Assay

Cell proliferation was determined using the Cell Proliferation ELISA kit, BrdU (Roche, 11669915001) following manufacturer's instructions. For more details, see Supplemental Information.

Transduction Buffer

5× Transduction Buffer

500 mM NaCl, 25 mM NaH_2PO4, 250 mM NDSB-201, 150 mM glycerol, 75 mM glycine, 1.25 mM $MgCl_2$, 1 mM 2-mercaptoethanol at pH 8.0. For more details, see Supplemental Information.

CRISPR/Cas9 Transduction Media

Opti-MEM media (Life Technologies) supplemented with 542 mM NaCl, 333 mM GABA, 1.67× N2, 1.67× B27, 1.67× non-essential amino acids, 3.3 mM Glutamine, 167 ng/ml bFGF2, and 84 ng/ml EGF. For more details on media preparation and catalog numbers, see Supplemental Information.

Recombinant Protein Production

His-tagged recombinant proteins were produced in *E. Coli* and purified using Ni-agarose affinity chromatography. Detailed methods and procedures are described in the Extended Experimental Procedures, as well as Tables S1 and S5.

Protein Transduction

We have established two transduction protocols that work best for most cell types and proteins to be transduced, typically yielding transduction efficiencies of 60%–90%. In the first protocol, transduction is performed for 12 hr at an osmolality of 500 mOsmol/kg (protocol 12/500). In brief, a day before protein transduction, cells were plated in the appropriate culture media without antibiotics. Next day, 5× transduction buffer with the protein of interest was mixed with cell culture media to obtain 1× transduction media at a tonicity of 500 mOsmol/kg and added to the cells. Cells were incubated for 12 hr, after which transduction media were removed and exchanged for regular culture media. In the second protocol, protein transduction is performed for 3 hr at an osmolality of 700 mOsmol/kg (protocol 3/700). Cells were plated as above. The next day, 1× transduction media with the protein of interest were added as above, and final osmolality was adjusted to 700 mOsmol/kg using NaCl. Cells were incubated for 3 hr, after which transduction media were removed and exchanged for regular culture media.

Beta-Lactamase Transduction and Quantification of Beta-Lactamase Incorporation

Beta-lactamase transduction in MEFs and mES cells was performed using the 3/700 and 12/500 protocol, respectively. After protein transduction, beta-lactamase activity was measured using the CCF2-AM loading kit (Life Technologies, K1032) following the manufacturer's instructions. Relative beta-lactamase activity was calculated using the following formula: relative beta-lactamase activity (%) = (X−B)/(A−B)*100, where X represents the beta-lactamase value of the sample; A is the beta-lactamase value of a reference sample, and B is the beta-lactamase value of cells transduced in isotonic media. For more details see Supplemental Information.

CRISPR-Cas9 Transduction

KBM7 cells were transduced with Cas9 protein and sgRNA with transduction media at 1,250 mOsmol/kg during 60 min in a 96-well format. In brief, 120,000 KBM7 cells were seeded per well using KBM7 media (IMDM supplemented with 10% FBS, non-essential amino acids, glutamax, 2-mercaptoethanol). The next day, 3 hr before transduction, cells were incubated 250 ng/ml of the interferon inhibitor B18R (eBiosciences). Then, cell culture media was removed and complete transduction mixture (10 μl of Cas9 in 5× transduction buffer, 30 μl of CRISPR/Cas9 transduction media, and 10 μl of sgRNA solution) was added to cells. sgRNA and DNA plasmid sequences are shown in Data S1, Data S2, and Data S3. Cells were incubated during 60 min at 37°C, and the transduction

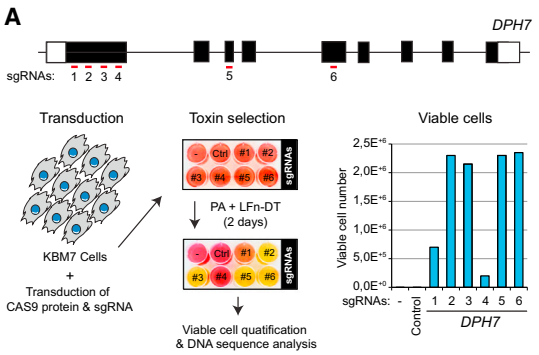

B

***DPH7* sgRNA #2;** 11 mutant sequences out of 11 sequences = 100%

```
ATGATGGGCTGTTTCGCCCTGCAAACGGTGGACACCGAGCTGACCGCGGACTCGGTGGAGTGGTGCCCGCTGCAAGGCT WT
ATGATGGGCTGTTTCGCCCTGCAAACGGTGGACACCGAGCTG=CCGCGGACTCGGTGGAGTGGTGCCCGCTGCAAGGCT D1
ATGATGGGCTGTTTCGCCCTGCAAACGGTGGACACCGAGCTGAC======TCGGTGGAGTGGTGCCCGCTGCAAGGCT D7 [3x]
ATGATGGGCTGTTTCGCCCTGCAAA==================CGGACTCGGTGGAGTGGTGCCCGCTGCAAGGCT D21
ATGATGGGCTGTTTCGCCCTGCAAACGGTGGA==========================GTGGTGCCCGCTGCAAGGCT D27

ATGATGGGCTGTTTCGCCCTGCAAACGGTGGACACCGAGCTGAACCGCGGACTCGGTGGAGTGGTGCCCGCTGCAAGGC +1 [4x]
ATGATGGGCTGTTTCGCCCTGCAAACGGTGGACACCGAGCTGATCCGCGGACTCGGTGGAGTGGTGCCCGCTGCAAGGC +1
```

***DPH7* sgRNA #6;** 12 mutant sequences out of 12 sequences = 100%

```
AGGGCAGCTCCACCTCCTGATGGTGAATGAGACGAGGCCCAGGCTGCAGAAAGTGGCCTCATGGCAGGCACATCAATTC WT
AGGGCAGCTCCACCTCCTGATGGTGAATGAGACGAGGCCCAGGCTGCAGAAAG=======TGGCAGGCACATCAATTC D8  [3x]
AGGGCAGCTCCACCTCCTGATGGTGAATGAGACGAGGCCCAGGCTGCAGAAAGC==========GCACATCAATTC D14/+1
AGGGCAGCTCCACCTCCTGATGGTGAATGAGACGAGGCCCAGGCTG==================CATCAATTC D24 [2x]
AGGGCAGCTCCACCTCCTGATGGTGAATGAGACGAGGCCCAGGCT----------------------CATCAATTC D25
AGGGCAGCTACACGTCCTG=================================ATGGCAGGCACATCAATTC D41
AG=================================================GGCACATCAATTC D64

AGGGCAGCTCCACCTCCTGATGGTGAATGAGACGAGGCCCAGGCTGCAGAAAGTGGCCTTCATGGCAGGCACATCAATT +1
AGGGCAGCTCCACCTCCTGATGGTGAATGAGACGAGGCCCAGGCTGCAGAAAGTGGCCCTCATGGCAGGCACATCAATT +1
TGTTTGGGAACCAGAAGA=================//==============GGCAGGCACATCAATTC D155
```

C

H1 hESCs

***DPH7* sgRNA #2;** 15 mutant sequences out of 15 sequences = 100%

```
ATGATGGGCTGTTTCGCCCTGCAAACGGTGGACACCGAGCTGACCGCGGACTCGGTGGAGTGGTGCCCGCTGCAAGGCT WT
ATGATGGGCTGTTTCGCCCTGCAAACGGTGGACACCGAGCT=ACCGCGGACTCGGTGGAGTGGTGCCCGCTGCAAGGCT D1
ATGATGGGCTGTTTCGCCCTGCAAACGGTGGACACCGAGCTGACCGCGGACTCGGTGGAGTGGTGCCCGCTGCAAGGCT D1
ATGATGGGCTGTTTCGCCCTGCAAACGGTGGACACCGAGCTGA=CCGCGGACTCGGTGGAGTGGTGCCCGCTGCAAGGCT D1
ATGATGGGCTGTTTCGCCCTGCAAACGGTGGACACCGAGC=======GGACTCGGTGGAGTGGTGCCCGCTGCAAGGCT D7
ATGATGGGCTGTTTCGCCCTGCAAACGGTGGACACCGAGCTGAC=======TCGGTGGAGTGGTGCCCGCTGCAAGGCT D7 [4x]
ATGATGGGCTGTTTCGCCCTGCAAACGGTGGA=========ACCGCGGACTCGGTGGAGTGGTGCCCGCTGCAAGGCT D10
ATGATGGGCTGTTTCGCCCTGCAAACGGTGGACACC==========GACTCGGTGGAGTGGTGCCCGCTGCAAGGCT D12
ATGATGGGCTGTTTCGCCCTGCAAACGGTGGACACCGAGCTGAC====TCC====TGGAGTGGTGCCCGCTGCAAGGCT D12/+3
ATGATGGGCTGTTTCGCCCTGCAAACGG==================ACTCGGTGGAGTGGTGCCCGCTGCAAGGCT D21
ATGATGGGCTGTTT=============================CGGACTCGGTGGAGTGGTGCCCGCTGCAAGGCT D32

ATGATGGGCTGTTTCGCCCTGCAAACGGTGAACACCGAGCTGAACCGCGGACTCGGTGGAGTGGTGCCCGCTGCAAGGC +2
ATGATGGGCTGTTTCGCCCTGCAAACGGTGGACACCGAGCTGAACCGCGGACTCGGTGGAGTGGTGCCCGCTGCAAGGC +1
```

***DPH7* sgRNA #6;** 18 mutant sequences out of 18 sequences = 100%

```
CCTCCTGATGGTGAATGAGACGAGGCCCAGGCTGCAGAAAGTGGCCTCATGGCAGGCACATCAATTCGAGGCCTGGATT WT
CCTCCTGATGGTGAATGAGACGAGGCCCAGGCTGCAGAAAGTGGC========AGGCACATCAATTCGAGGCCTGGATT D8 [7x]
CCTCCTGATGGTGAATGAGACGAGGCCCA================CTCATGGCAGGCACATCAATTCGAGGCCTGGATT D16
CCTCCTGATGGTGAATGAGACGAGGCC==================CCTCATGGCAGGCACATCAATTCGAGGCCTGGATT D18
CCTCCTGATGGTGAATGAGACGAGGCCCAGGCTGC----------------CACATCAATTCGAGGCCTGGATT D21
CCTCCTGATGGTGAATGAGACGAGGCCCAGGCTGCAGAAAGT----------------------GGCCTGGATT D27
CCTCCTGATGGTGAATGAGACGAGGCC-------------------------------AGGCCTGGATT D41

CCTCCTGATGGTGAATGAGACGAGGCCCAGGCTGCAGAAAGTGGCCCTCATGGCAGGCACATCAATTCGAGGCCTGGAT +1
CCTCCTGATGGTGAATGAGACGAGGCCCAGGCTGCAGAAAGTGGCCTTCATGGCAGGCACATCAATTCGAGGCCTGGAT +1
CCTCCTGATGGTGAATGAGACGAGGCCCAGGCTGCAGAAAGTGGCCCTCATGGCAGGCACATCAATTCGAGGCCTGGAT +1
CCTCCTGATGGTGAATGAGACGAGGCCCAGGCTGCAGAAAGTG==CAGGCACA=TCATGGCAGGCACATCAATTCGAGG D3/+8
CCTCCTGATGGTGAATGAGACGAGGCCCAGGCTGCAGAAAGTGGC==AGGCACATCTGCAGAAAGTGGCAGAAAG==TG D4/+28
CCTCCTGATGGTGAATGAGACGAGGCCCAGGCTGCAGAAAGTGGC===AGGCACATCAATT===GCAGGCACATCAATTC D6/+13
```

D

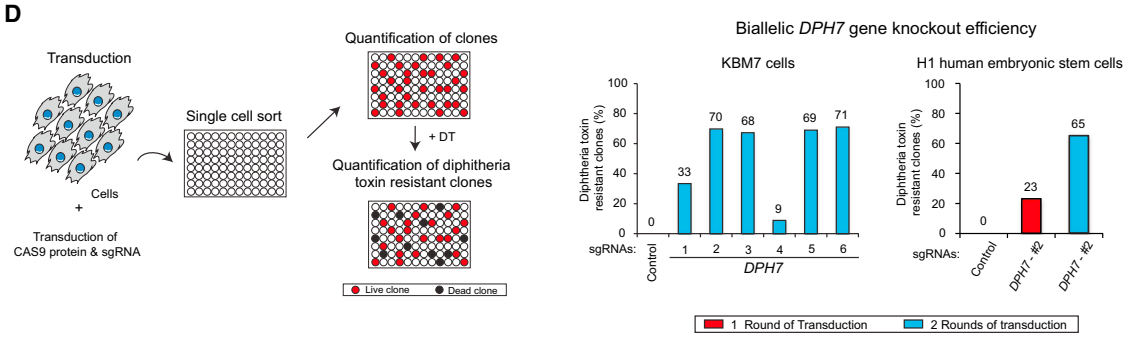

E

KBM7 cells

***DPH7* Knockout clones - sgRNA #2**

```
                TTTCGCCCTGCAAACGGTGGACACCGAGCTGACCGCGGACTCGGTGGAGTGGTGCCCGCTGCAAGGCTGCAGGCA WT
Clone
#201 |A1-TTTCGCCCTGCAAACGGTGGACACCGAGC======GGACTCGGTGGAGTGGTGCCCGCTGCAAGGCTGCAGGCA D7
     |A2-TTTCGCCCTGCAAACGGTGGACACCG=========CGGACTCGGTGGAGTGGTGCCCGCTGCAAGGCTGCAGGCA D9

#202 |A1-TTTCGCCCTGCAAACGGTGGACACCGAGCTGAACCGCGGACTCGGTGGAGTGGTGCCCGCTGCAAGGCTGCAGGC +1
     |A2-TTTCGCCCTGCAAACGGTGGACACCGAGCTGACCGCGGACTCGGTGGAGTGGTGCCCGCTGCAAGGCTGCAGGCA +75
       AACTAGCCCTGAAAATGGATGGCGCTGGAGCGTCGGGCCCATACCCGGCCGTCGCCGGCAGTCGAGAGTGGACGG

#203 |A1-TTTCGCCCTGCAAACGGTGGACAC==========GGACTCGGTGGAGTGGTGCCCGCTGCAAGGCTGCAGGCA D12
     |A2-TTTCGCCCTGCAAACGGTGGACACCG=========CGGACTCGGTGGAGTGGTGCCCGCTGCAAGGCTGCAGGCA D9
```

***DPH7* Knockout clones - sgRNA #5**

```
Clone
#501 |A1-TCCTCAGGTGTCACATCCCGGTGGCTGGACATGCCCTCTTGGGCTTGGCAGATGCCAGTGGATCCATACAACTGC D19
     |A2-TCCTCAGGTGTCACATCCCGGTGGCTGGACATGCCCTCT=======//=========GAAGTGACAGGATGTTCA D276

#502 |A1-TCCTCAGGTGTCACATCCCGGTGGCTGGACATGCCCTCT=GGGCTTGGCAGATGCCAGTGGATCCATACAACTGC D1
     |A2-TCCTCAGGTGTCACATCCCGGTGGCTGGACATGCCCTCTTGGGCTTGGCAGATGCCAGTGGATCCATACAACTGC +59
       CTGGCATGCACCTGTAATTACAGCTACTGTCTGTGCATCTAACCATTTTGTCAATCCAC

#503 |A1-TCCTCAGGTGTCACATCCCGGTGGCTGGACATGCCCT========TGGCAGATGCCAGTGGATCCATACAACTGC D8
     |A2-CTAAGAGCTC=============//==============GGGCTTGGCAGATGCCAGTGGATCCATACAACTGC D606
```

***DPH7* Knockout clones - sgRNA #3**

```
          CGGACTCGGTGGAGTGGTGCCCGCTGCAAGGCTGCAGGCACCCTGCTGGCGTGCGGGACCTACCAGCTGCGGCGGC WT
Clone
#301 |A1-CGGACTCGGTGGAGTGGTGCCCGCTGCAAGGCC=CAGGCACCTGCTGGCGTGCGGGACCTACCAGCTGCGGCGGC D2/+1
     |A2-CGGACTCGGTGGAGTGGTGCCCGCTGCA=======GGCACCTGCTGGCGTGCGGGACCTACCAGCTGCGGCGGC D8

#302 |A1-CGGACTCGGTGGAGTGGTGCCCGCTGCA=======AGGCACCTGCTGGCGTGCGGGACCTACCAGCTGCGGCGGC D7
     |A2-CGGACTCGGTGGAGTGGTGCCCGCTGCAAGGC================GTGCGGGACCTACCAGCTGCGGCGGC D17

#303 |A1-CGGACTCGGTGGAGTGGTGCCCGCTGCAAGGC=======ACCTGCTGGCGTGCGGGACCTACCAGCTGCGGCGGC D7
     |A2-CGGACTCGGTGGAGTGGTGCCCGCTGCA========GGCACCTGCTGGCGTGCGGGACCTACCAGCTGCGGCGGC D8
```

***DPH7* Knockout clones - sgRNA #6**

```
Clone
#601 |A1-CCTGATGGTGAATGAGACGAGGCCCAGGCTGCAGAAAGTGGCC=======AGGCACATCAATTCGAGGCCTGGAT D8
     |A2-CCTGATGGTGAATGAGACGAGGCCCAGGCTGCAGAAAGTGGC=======CAGGCACATCAATTCGAGGCCTGGAT D7

#602 |A1-CCTGATGGTGAATGAGACGAGGCCCAGGCTGCAGAAAGTGGCA========GCACATCAATTCGAGGCCTGGAT D10/+1
     |A2-CCTGATGGTGAATGAGACGAGGCC=========================CAGGCACATCAATTCGAGGCCTGGAT D25

#603 |A1-CCTGATGGTGAATGAGACGAGGCCCAGGCTGCAG==============CAGGCACATCAATTCGAGGCCTGGAT D15
     |A2-CCTGATGGTGAATGAGACGAGGCCCAGGCTGCAGAAAGTGGCCAATCATGGCAGGCACATCAATTCGAGGCCTGG +2
```

H1 hESCs

***DPH7* Knockout clones - sgRNA #2**

```
                TTTCGCCCTGCAAACGGTGGACACCGAGCTGACCGCGGACTCGGTGGAGTGGTGCCCGCTGCAAGGCTGCAGGCA WT
Clone
# 01 |A1-TTTCGCCCTGCAAACGGTGGAC==================TCGGTGGAGTGGTGCCCGCTGCAAGGCTGCAGGCA D18
     |A2-TTTCGCCCTGCAAACGGTGGACACCGA=============================GCTGCAAGGCTGCAGGCA D30

# 02 |A1-TTTCGCCCTGCAAACGGTGGACACC=====GACCGCGGACTCGGTGGAGTGGTGCCCGCTGCAAGGCTGCAGGCA D5
     |A2-TTTCGCCCTGCAAACGGTGGACACCGAGCTGAACCGCGGACTCGGTGGAGTGGTGCCCGCTGCAAGGCTGCAGGC +1

# 03 |A1-TTTCGCCCTGCAAACGGTGGACACCGAGCTG=CCGCGGACTCGGTGGAGTGGTGCCCGCTGCAAGGCTGCAGGCA D1
     |A2-TTTCGCCCTGCAAACGGTGGACACCGAGCTGAACCGCGGACTCGGTGGAGTGGTGCCCGCTGCAAGGCTGCAGGC +1

# 04 |A1-TTTCGCCCTGCAAACGGTGGACACCGAGCTGAACCGCGGACTCGGTGGAGTGGTGCCCGCTGCAAGGCTGCAGGC +1
     |A2-TTTCGCCCTGCAAACGGTGGACACCG=========CGGACTCGGTGGAGTGGTGCCCGCTGCAAGGCTGCAGGCA D9/+51
```

```
                TTTCGCCCTGCAAACGGTGGACACCGAGCTGACCGCGGACTCGGTGGAGTGGTGCCCGCTGCAAGGCTGCAGGCA WT
Clone
# 05 |A1-TTTCGCCCTGCAAACGGTGGACACCGAGCTGACTCGGTGGAGTCAGCTC//CACCGAGCTGACTCGCCCGCTGCA +140
     |A2-TTTCGCCCTGCAAACGGTGGACACCGAGCTGACACCGCGGACTCGGTGGAGTGGTGCCCGCTGCAAGGCTGCAGG +2

# 06 |A1-TTTCGCCCTGCAAACGGTGGACACCGAGTCAGGTGACTCGCCCTGCAAACGGTGGACTCGGTGGAGTGGTGCCCG D8/+25
     |A2-TTTCGCCCTGCAAACGGTGGACACCGAG==============GTGGAGTGGTGCCCGCTGCAAGGCTGCAGGCA D15

# 07 |A1-TTTCGCCCTGCAAACGGTGGACACCGAGCTGATCCGCGGACTCGGTGGAGTGGTGCCCGCTGCAAGGCTGCAGGC +1
     |A2-TTTCGCCCTGCAAACGGTGGACACCGAGCTGAACCGCGGACTCGGTGGAGTGGTGCCCGCTGCAAGGCTGCAGGC +1

# 08 |A1-TTTCGCCCTGCAAACGGTGGACACCGAGCTGAC====TCGGTG==GGAGTGGTGCCCGCTGCAAGGCTGCAGGCA D12/+6
     |A2-TTTCGCCCTGCAAACGGTGGACACCGAGCTGAC=======TCGGTGGAGTGGTGCCCGCTGCAAGGCTGCAGGCA D7
```

(legend on next page)

media was carefully replaced by standard culture media supplemented with 250 ng/ml of B18R. Cells were incubated for 48 hr and analyzed by flow cytometry. Knockout of endogenous *DPH7* gene was determined by adding LFn-DT (Carette et al., 2009) and DNA sequencing of the surviving cells. Two rounds of Cas9/sgRNA transduction were performed as above with a recovery time between transductions of 5–7 days. See Tables S3 and S4 for primer sequences for genomic DNA amplification and surveyor assay.

H1 human ESCs were transduced as above with slight modifications. Cells were passaged by mechanical dissociation into small clumps following mTeSR1 manufacturer's instructions and seeded on a matrigel-coated plate. Cells were transduced 2–3 days after seeding when they reached a confluency of 80%–90%. Two rounds of Cas9/sgRNA transduction were performed the same as above with a recovery time between transductions of 5–7 days. Cells were not passaged between two transductions.

SUPPLEMENTAL INFORMATION

Supplemental Information includes Extended Experimental Procedures, six figures, five tables, and three data files and can be found with this article online at http://dx.doi.org/10.1016/j.cell.2015.03.028.

AUTHOR CONTRIBUTIONS

D.S.D. conceived the project, designed and performed all experiments, interpreted the results, and wrote the manuscript. R.J.P. helped to set up and execute imaging-based quantification of macropinocytosis and vesicle release, and A.P performed imaging experiments, aided with data analysis. W.R.K. and H.C. helped with the culture and transduction of gut organoids, and V.P. generated the Nhe1 knockout cells. R.J.L. helped with the setup of the CRISPR/Cas system. H.R. helped with recombinant protein synthesis, and N.G. conceived and directed the project, designed experiments, interpreted the results, and wrote the manuscript.

ACKNOWLEDGMENTS

The authors thank Sarah Opitz for critically reading the manuscript; Nune Schelling for technical support; Stefan van der Elst of the Hubrecht Institute FACS facility for help with cell sorting; Anko de Graaf of the Hubrecht Institute imaging facility; David Egan of the Cell Screening facility at the UMCU; Gustavo Mostoslavsky for providing lentiviral vectors; Saravanan Manikam and Antoinette Killian for help with NDSB analysis; Thijn Brummelkamp for providing the KBM7 cells; Liqun Luo and Paul Krimpenfort for providing mTmG reporter mice; and Bart van Steen and Jack den Hartog for help with compound synthesis. This work was funded in part by The Netherlands Organization for Scientific Research (NWO, project 91796323 and 91610138, and American Heart Association 11BGIA7720005). D.S.D. and N.G. are co-inventors on a patent application describing the transduction technology PCT/IB2014/064127 and co-founders of NTrans technologies.

Received: October 28, 2014
Revised: December 19, 2014
Accepted: March 12, 2015
Published: April 23, 2015

REFERENCES

Boyer, L.A., Lee, T.I., Cole, M.F., Johnstone, S.E., Levine, S.S., Zucker, J.P., Guenther, M.G., Kumar, R.M., Murray, H.L., Jenner, R.G., et al. (2005). Core transcriptional regulatory circuitry in human embryonic stem cells. Cell *122*, 947–956.

Carette, J.E., Guimaraes, C.P., Varadarajan, M., Park, A.S., Wuethrich, I., Godarova, A., Kotecki, M., Cochran, B.H., Spooner, E., Ploegh, H.L., and Brummelkamp, T.R. (2009). Haploid genetic screens in human cells identify host factors used by pathogens. Science *326*, 1231–1235.

Charpentier, E., and Doudna, J.A. (2013). Biotechnology: Rewriting a genome. Nature *495*, 50–51.

Commisso, C., Flinn, R.J., and Bar-Sagi, D. (2014). Determining the macropinocytic index of cells through a quantitative image-based assay. Nat. Protoc. *9*, 182–192.

Kim, S., Kim, D., Cho, S.W., Kim, J., and Kim, J.S. (2014). Highly efficient RNA-guided genome editing in human cells via delivery of purified Cas9 ribonucleoproteins. Genome Res. *24*, 1012–1019.

Kültz, D., Madhany, S., and Burg, M.B. (1998). Hyperosmolality causes growth arrest of murine kidney cells. Induction of GADD45 and GADD153 by osmosensing via stress-activated protein kinase 2. J. Biol. Chem. *273*, 13645–13651.

Louis, S.A., and Reynolds, B.A. (2005). Generation and differentiation of neurospheres from murine embryonic day 14 central nervous system tissue. Methods Mol. Biol. *290*, 265–280.

Lundberg, M., and Johansson, M. (2001). Is VP22 nuclear homing an artifact? Nat. Biotechnol. *19*, 713–714.

Mortensen, M., Ebert, B., Wafford, K., and Smart, T.G. (2010). Distinct activities of GABA agonists at synaptic- and extrasynaptic-type GABAA receptors. J. Physiol. *588*, 1251–1268.

Okada, C.Y., and Rechsteiner, M. (1982). Introduction of macromolecules into cultured mammalian cells by osmotic lysis of pinocytic vesicles. Cell *29*, 33–41.

Paz, I., Sachse, M., Dupont, N., Mounier, J., Cederfur, C., Enninga, J., Leffler, H., Poirier, F., Prevost, M.C., Lafont, F., and Sansonetti, P. (2010). Galectin-3, a marker for vacuole lysis by invasive pathogens. Cell. Microbiol. *12*, 530–544.

Figure 7. Endogenous Gene Disruption Induced by CRISPR-Cas9 Transduction

(A) Top: schematic depiction of the *DPH7* gene and target sites of six different sgRNAs used in the experiments. Bottom: schematic depiction of the Cas9-sgRNA transduction and diphtheria toxin selection procedure. KBM7 cells were transduced twice with Cas9 and *DPH7* sgRNAs with a 7 day interval between transductions. Controls were untreated cells and cells transduced with Cas9 together an AAVS1 sgRNA (Crtl). 7 days after the second transduction, cells were treated with LFn-DTA. Bar graph shows the number of viable cells after 2 days of diphtheria toxin selection.

(B) Analysis of target-site mutations in the endogenous *DPH7* gene in diphtheria-toxin-resistant KBM7 cells after transduction of recombinant Cas9 protein and in-vitro-transcribed sgRNA. The wild-type (WT) sequence is shown at the top. Start codon is indicated with underlined ATG. Deletions are indicated by dashes and yellow background and insertions with underlined green text. The sizes of the insertions (+) or deletions (D) are indicated to the right of each mutated site. Numbers in brackets show the amount of sequences obtained. In the wild-type sequences are indicated the sgRNA binding site and PAM sequence in underlined red and blue text, respectively. The primers used to amplify the different DPH7 genomic regions are listed in Table S3.

(C) Analysis of target-site mutations at endogenous *DPH7* gene in diphtheria toxin-resistant H1 hESCs after transduction of recombinant Cas9 protein and in-vitro-transcribed *DPH7* sgRNAs. Annotation as in (B).

(D) Schematic representation of the experimental design used for the quantification of biallelic *DPH7* gene knockout by Cas9-sgRNA transduction. KBM7 or hESCs were transduced once or twice (as indicated) with Cas9 together with *DPH7* sgRNAs. Control was cells transduced with Cas9 and an AAVS1 sgRNA. After 3 days, single cells were sorted into 384-well plates using a flow cytometer. 7 days later, the number of expanding clones was counted, and cells were treated with diphtheria toxin. After 2 days of diphtheria toxin treatment, surviving clones were counted. *DPH7* knockout efficiency was calculated as the percentage of total single-cell clones that were diphtheria toxin resistant of total clones obtained.

(E) Biallelic DNA sequence analysis of diphtheria toxin-resistant clones in KBM7 cells and H1 hESCs. Annotation as in (B). A1, allele 1; A2, Alele2. The sizes of the insertions (+) or deletions (D) are indicated to the right of each mutated site.

Ramakrishna, S., Kwaku Dad, A.B., Beloor, J., Gopalappa, R., Lee, S.K., and Kim, H. (2014). Gene disruption by cell-penetrating peptide-mediated delivery of Cas9 protein and guide RNA. Genome Res. *24*, 1020–1027.

Ray, K., Bobard, A., Danckaert, A., Paz-Haftel, I., Clair, C., Ehsani, S., Tang, C., Sansonetti, P., Tran, G.V., and Enninga, J. (2010). Tracking the dynamic interplay between bacterial and host factors during pathogen-induced vacuole rupture in real time. Cell. Microbiol. *12*, 545–556.

Redon, C.E., and Bonner, W.M. (2011). High salt and DNA double-strand breaks. Proc. Natl. Acad. Sci. USA *108*, 20281–20282.

Sato, T., Vries, R.G., Snippert, H.J., van de Wetering, M., Barker, N., Stange, D.E., van Es, J.H., Abo, A., Kujala, P., Peters, P.J., and Clevers, H. (2009). Single Lgr5 stem cells build crypt-villus structures in vitro without a mesenchymal niche. Nature *459*, 262–265.

Schwarze, S.R., Hruska, K.A., and Dowdy, S.F. (2000). Protein transduction: unrestricted delivery into all cells? Trends Cell Biol. *10*, 290–295.

Srinivas, S., Watanabe, T., Lin, C.S., William, C.M., Tanabe, Y., Jessell, T.M., and Costantini, F. (2001). Cre reporter strains produced by targeted insertion of EYFP and ECFP into the ROSA26 locus. BMC Dev. Biol. *1*, 4.

Tomilin, A., Reményi, A., Lins, K., Bak, H., Leidel, S., Vriend, G., Wilmanns, M., and Schöler, H.R. (2000). Synergism with the coactivator OBF-1 (OCA-B, BOB-1) is mediated by a specific POU dimer configuration. Cell *103*, 853–864.

Vuillard, L., Braun-Breton, C., and Rabilloud, T. (1995). Non-detergent sulphobetaines: a new class of mild solubilization agents for protein purification. Biochem. J. *305*, 337–343.

Zhou, J., Fan, J., and Hsieh, J.T. (2006). Inhibition of mitogen-elicited signal transduction and growth in prostate cancer with a small peptide derived from the functional domain of DOC-2/DAB2 delivered by a unique vehicle. Cancer Res. *66*, 8954–8958.

Zuris, J.A., Thompson, D.B., Shu, Y., Guilinger, J.P., Bessen, J.L., Hu, J.H., Maeder, M.L., Joung, J.K., Chen, Z.-Y., and Liu, D.R. (2014). Cationic lipid-mediated delivery of proteins enables efficient protein-based genome editing in vitro and in vivo. Nat. Biotech. *33*, 73–80.